Observation and first properties measurements of the Higgs boson candidate in its di-photon decay with the ATLAS experiment

Marine Kuna
INFN Sezione di Roma

Seminar Roma
July 4, 2013

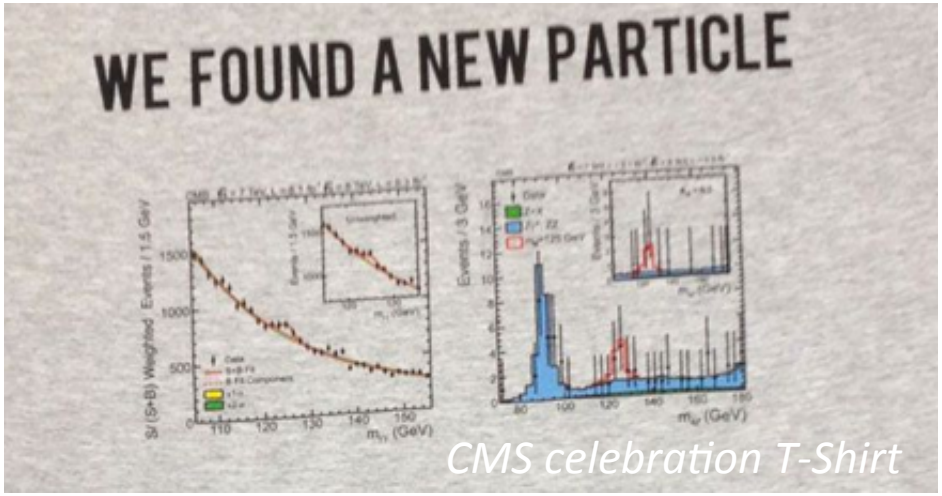

CMS celebration T-Shirt


François Englert & Peter Higgs

July 4th: Anniversary of a Discovery Announcement


CERN main auditorium

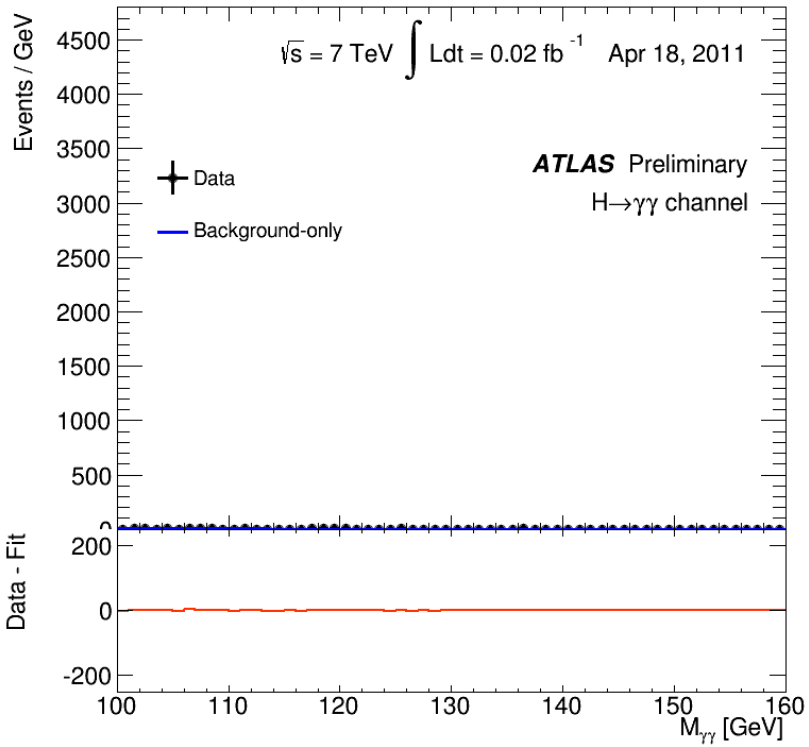

Why the Higgs ?

- Standard Model of Particle Physics:
  - 6 quarks, 6 leptons, bosons: strong interaction (gluons) and electroweak (photon, Z°, W^+, W^-)
- Gauge bosons Z°, W^+, W^- have masses (resp. 91 and 80 GeV) → Electro-Weak Symmetry breaking:
  - Solution is introduction of a massive scalar particle (electric charge & spin = 0): the Higgs Boson

The Higgs boson is the only elementary particle from the Standard Model that had not been experimentally observed prior to last year.

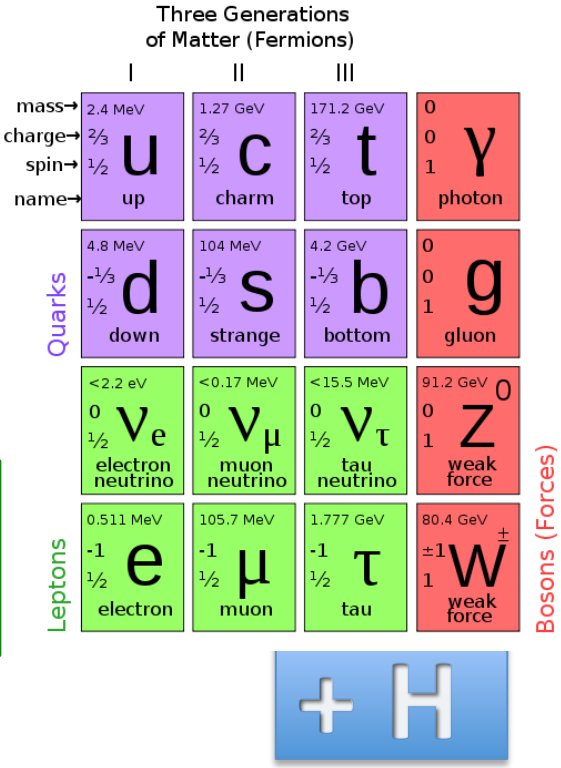

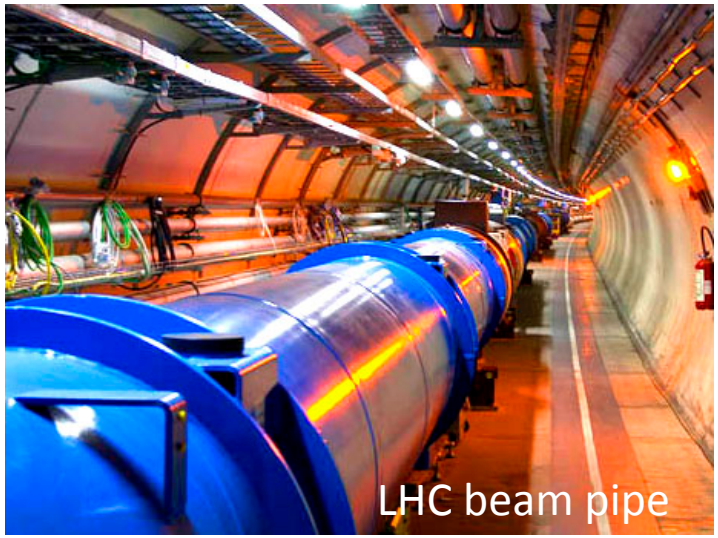

- Its search has been one of the motivations the construction of the Large Hadron Collider, among an otherwise vast physics program (search for super-symmetry & dark matter candidates, CP symmetry breaking, nature and properties of quark-gluon plasma…)

SM Higgs Boson Production at the LHC

gluon fusion (ggF)

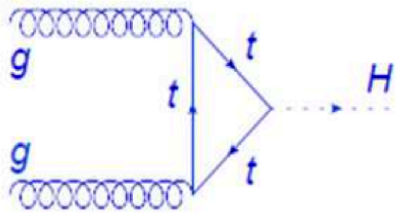

19.5 pb (87%)

vector boson fusion (VBF)

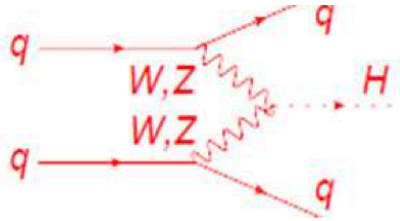

1.6 pb (7%)

associated production with W/Z (WH, ZH)

1.1 pb (5%)

associated production with top anti-top pairs (ttH)

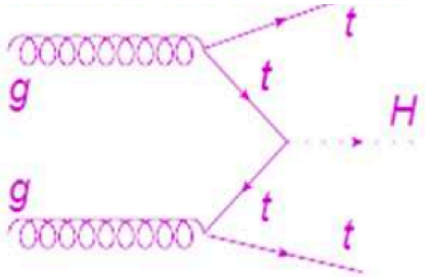

0.1 pb (1%)

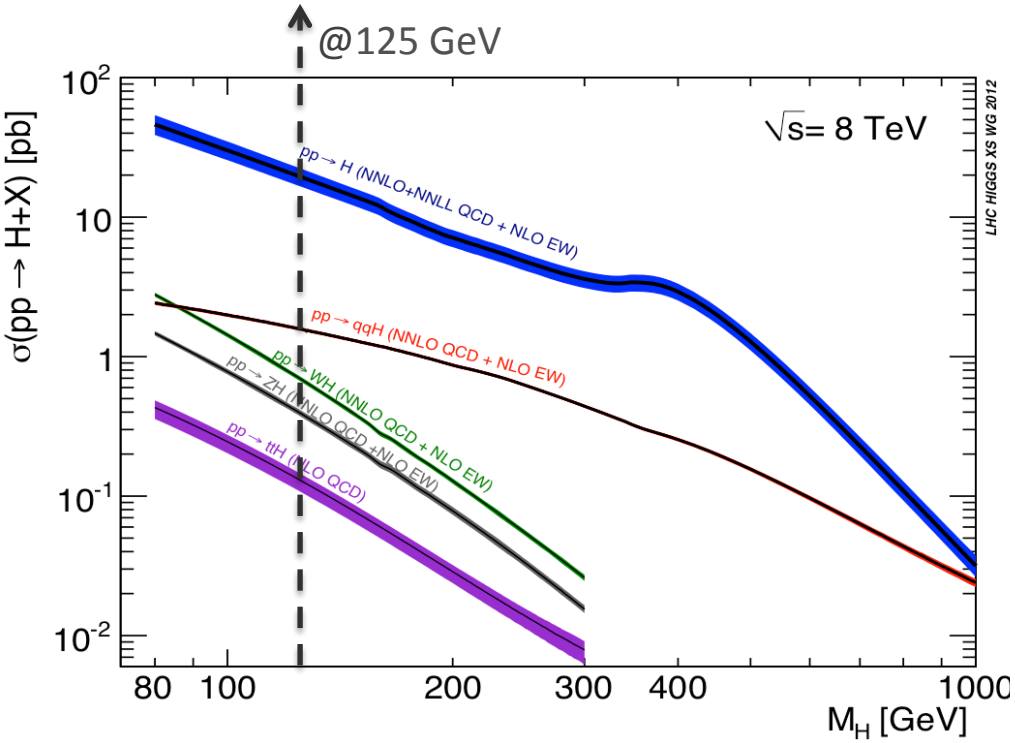

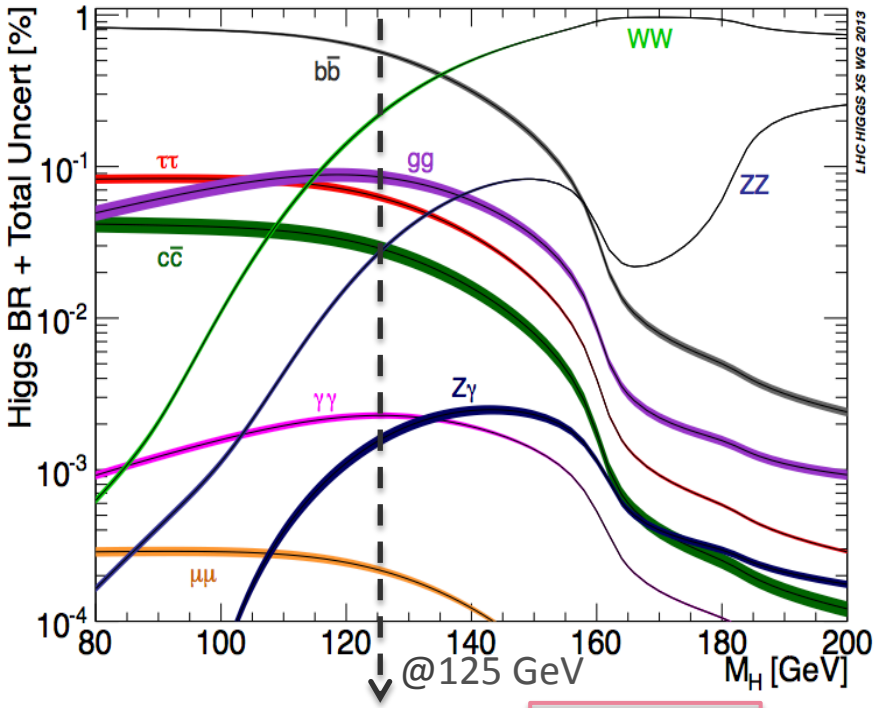

Branching ratios @125 GeV: bb (57.7%); WW (21.5%); ττ (6.3%); ZZ (2.6%); γγ (0.23%)

The ATLAS Experiment

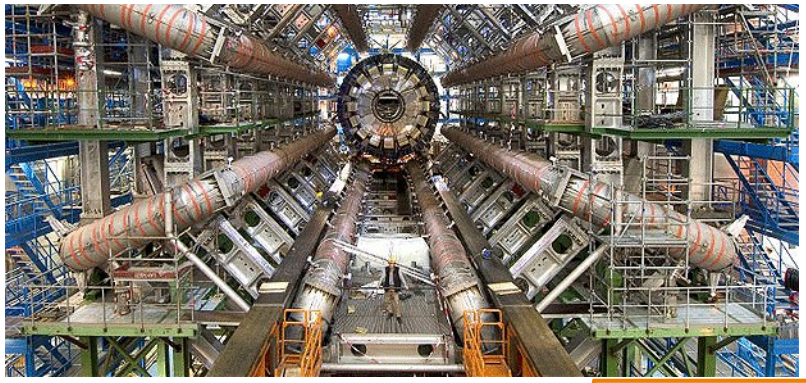

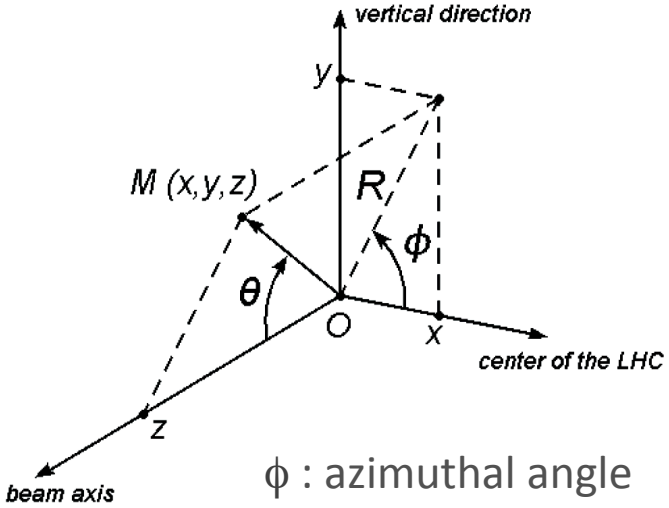

ϕ : azimuthal angle

η = - ln [tan (θ/2)]

Muon Spectrometer

Hadronic Calorimeter

Electromagnetic Calorimeter

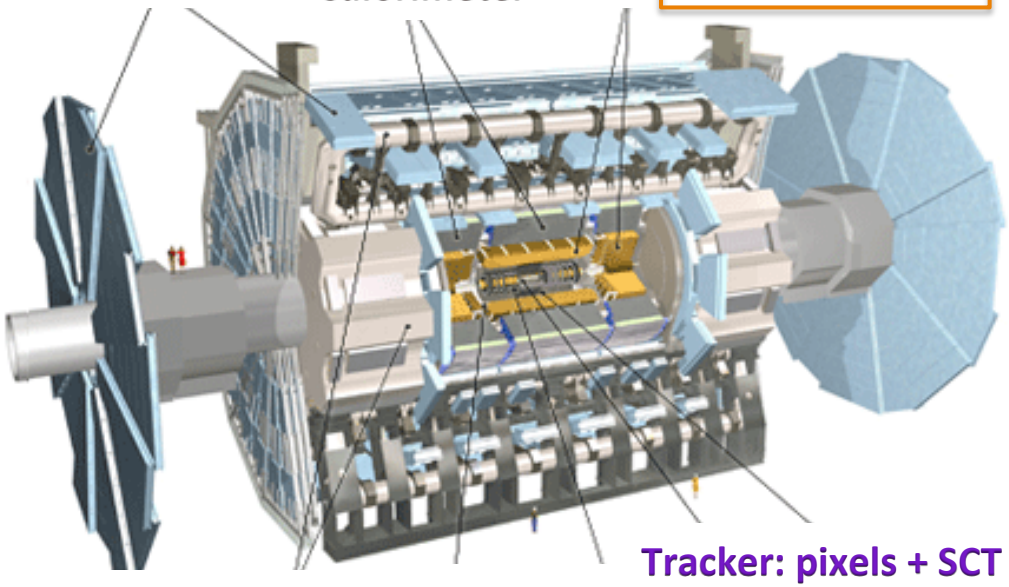

Toroidal Coils

Solenoidal Coil

Tracker: pixels + SCT (precision)+ Transition Radiation Tracker

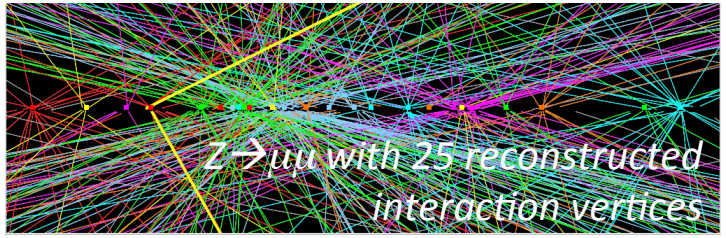

Average number of interactions per bunch crossing: from 10 (7 TeV) to 20 (8 TeV)

Instantaneous luminosity up to $7.7 \times 10^{33} cm^{-2} s^{-1}$

→ Many challenges to meet at the trigger and performance level

+ 3 Level Trigger System

EM Calorimeter

Liquid Argon-Lead sampling calorimeter

- Accordion geometry for azimuthal hermeticity
- High longitudinal and lateral granularity (175000 cells)

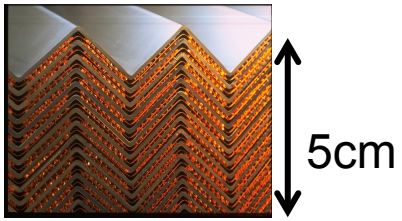

Energy Resolution

Sampling/stochastic term (statistical variations of the shower shape)

Noise term (electronics, pile-up)

Constant term (non uniformities, calibration imperfections)

$$\frac{\sigma_E}{E} = \frac{a}{\sqrt{E}} \oplus \frac{b}{E} \oplus c$$

ATLAS specifications: a ≃ 10%, b ≃ 170 MeV and c = 0.7% (CMS : a ≃ 2.8%, c ≃ 0.3%)

Energy Reconstruction

X sum of E in cells

$$\begin{cases} E_{tot} = E_{cal} + E_{front} + E_{back} \\ E_{cal} = C_{cal}(X,\eta)(1 + f_{out}(X,\eta))E_{clus} \\ E_{front} = a(E_{cal},\eta) + b(E_{cal},\eta)E_{PS} + c(E_{cal},\eta)E_{PS}^2 \\ E_{back} / E_{cal} = f_{leak} = f_0^{leak}(\eta)X + f_1^{leak}(\eta)e^X \end{cases}$$

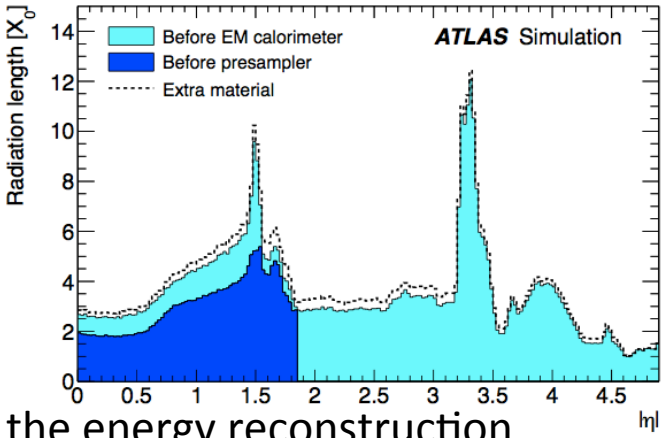

→ Upstream material knowledge central problem of the energy reconstruction (Monte Carlo coefficients depending on the detector simulation)

Event selection

Di-photon Trigger

EM clusters
E_T > 35, 25 GeV
Efficiency >99%
wrt offline
selection

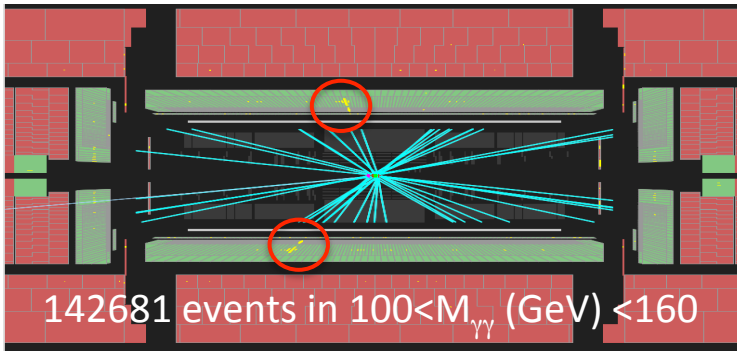

Kinematic cuts

$p_T^{\gamma 1}$, $p_T^{\gamma 2}$> 40, 30 GeV, η<2.47

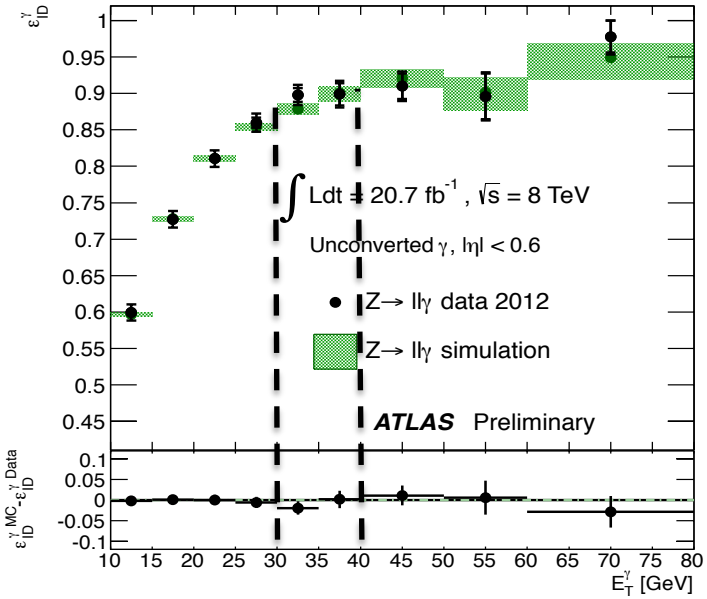

Photon identification efficiency measured on radiative Z→llγ decays

Photon identification

Shower shape variables: exploit the fine segmentation of the EM calorimeter

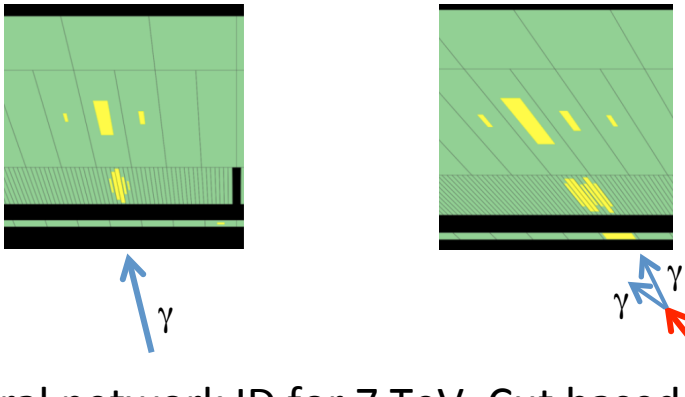

Neural network ID for 7 TeV, Cut based for 8 TeV

Photon track and calorimetric isolation

$$\Delta R = \sqrt{(\Delta\eta)^2 + (\Delta\varphi)^2}$$

Σ p_T^{tracks} < 2.6 GeV in ΔR<0.2
Σcalo energy < 6 GeV in ΔR<0.4

Corrected for underlying events

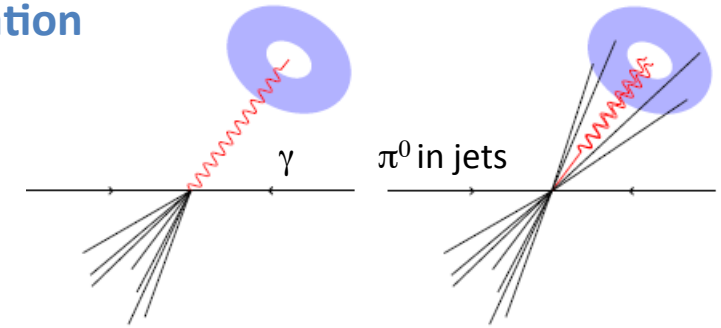

→ ε_{event}~40%

Background rejection (1)

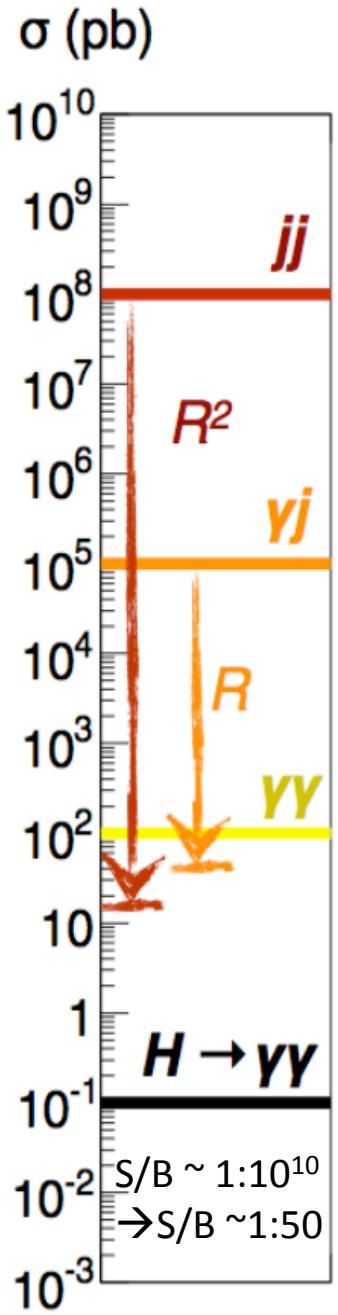

jj where both jets are mis-identified as a photon due to hard π^0

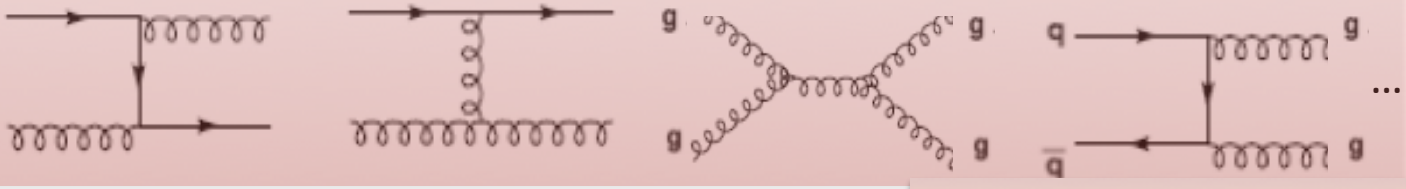

reducible backgrounds

γj where the jet is mis-identified as a photon

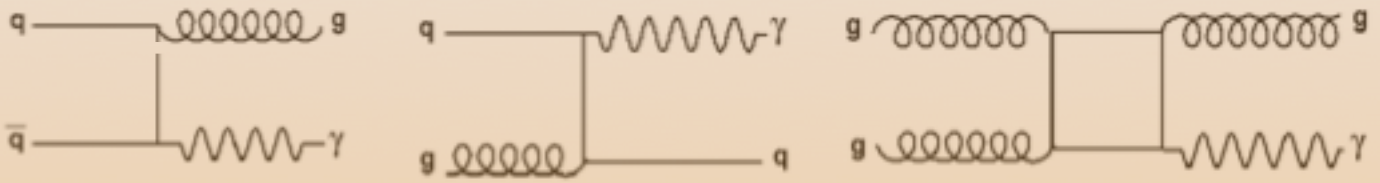

irreducible background

QCD γγ

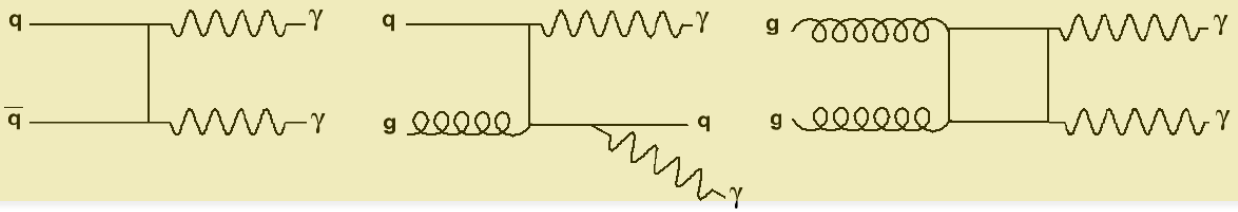

+ Drell-Yan, γ+Z/W: ~ $O(10^{-1})$ × $\sigma_{\gamma\gamma}$ electrons identified as photons

H→ γγ (signal)

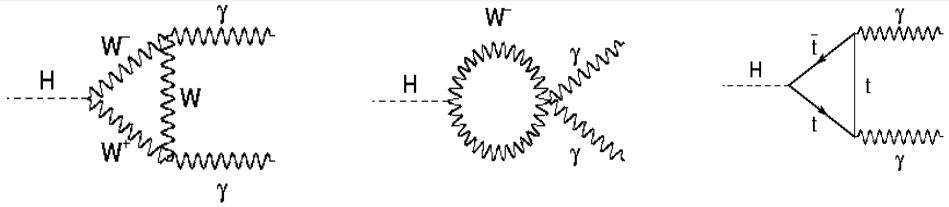

Background rejection (2)

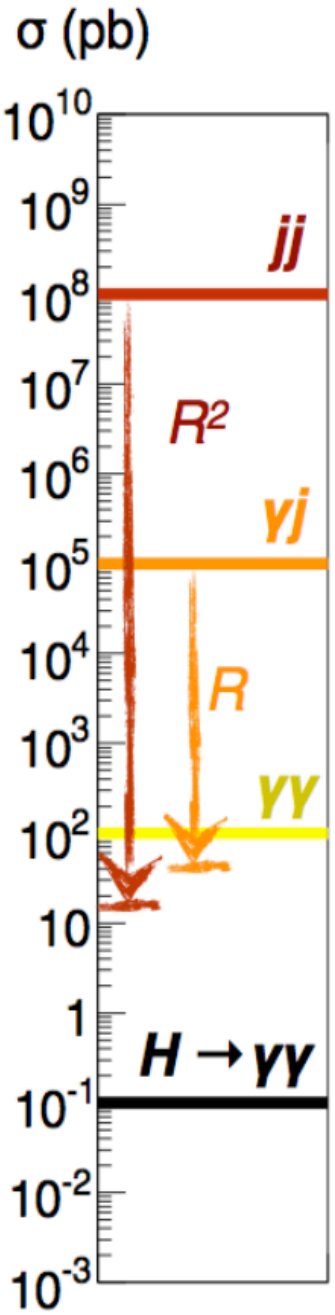

- Background composition derived with 4 different data-driven methods using control regions relaxing the identification or the isolation criteria
- 2D fit of the 1st and 2nd photon isolation spectrum
  - jet isolation pdf: non identified data sample
  - photon pdf: fully identified sample - data-driven background contamination

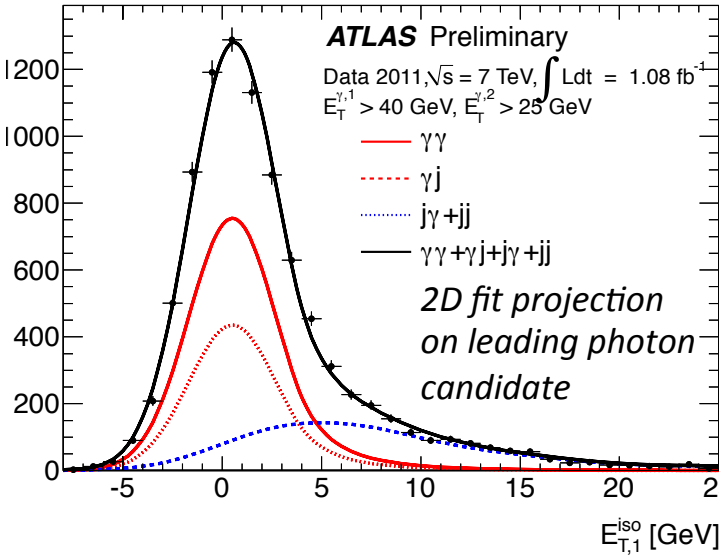

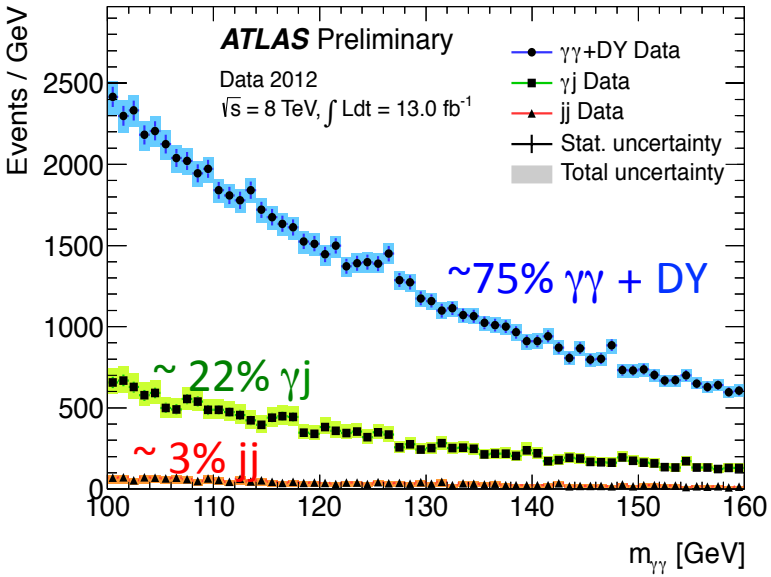

→ Data sample purity ~75%

→ Invariant mass $M_{\gamma\gamma}$ is the discriminating variable for the H→γγ analysis

Mass Resolution (1)

$$M_{\gamma\gamma}^2 = 2\,p_T^{\gamma_1}\,p_T^{\gamma_2}\left[\cosh(\eta_1-\eta_2)-\cos(\varphi_1-\varphi_2)\right]$$

$M_{\gamma\gamma}$ overall resolution: 1.7 GeV

Photon energy scale extrapolated from electrons from Z

~1.2-1.8% additional smearing term in energy resolution for MC calibration to match data Z lineshape

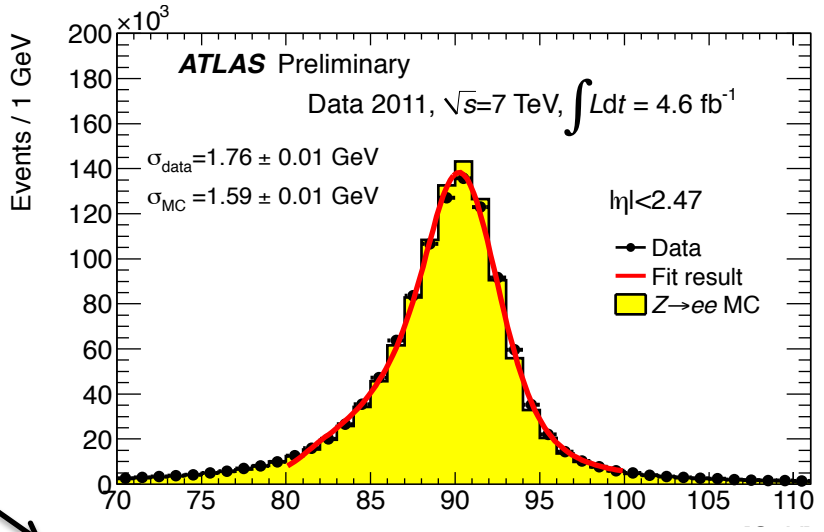

Stability of EM calorimeter response vs time and pile-up <0.1%

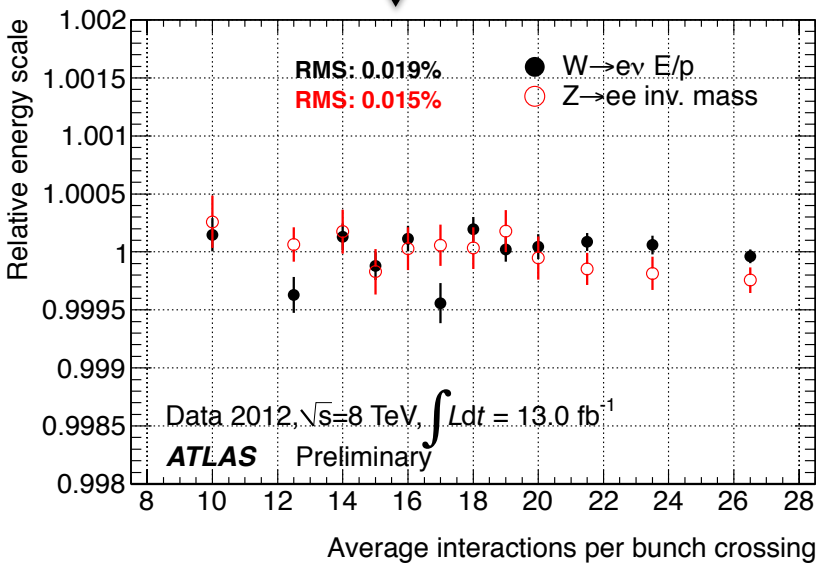

Resolution stable with pile-up

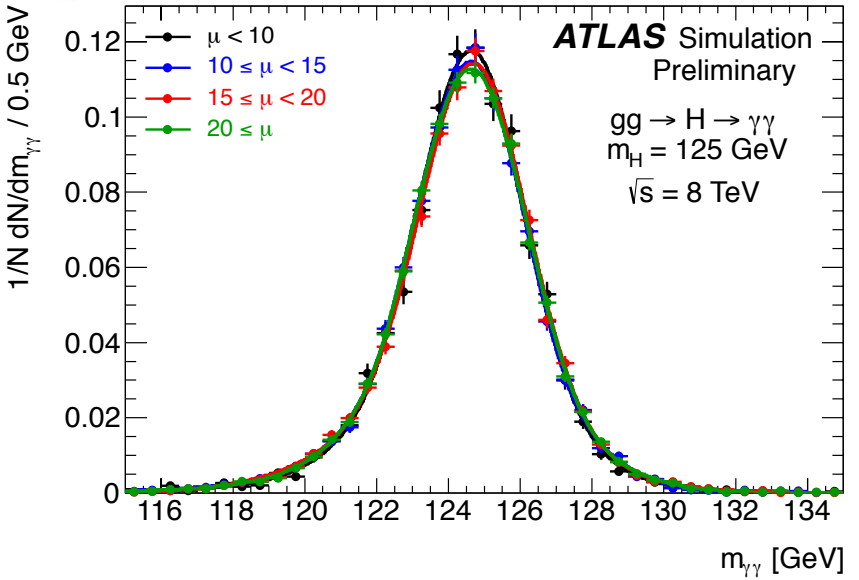

Mass Resolution (2)

$$M_{\gamma\gamma}^2 = 2 p_T^{\gamma_1} p_T^{\gamma_2} \left[\cosh(\eta_1 - \eta_2) - \cos(\varphi_1 - \varphi_2)\right]$$

Vertex determination → Di-photon angle reconstruction

Resolution of angle measurement dominated by reconstruction of primary vertex *z* position (IP spread of ~5.6 cm would add ~1.4 GeV in mass resolution)

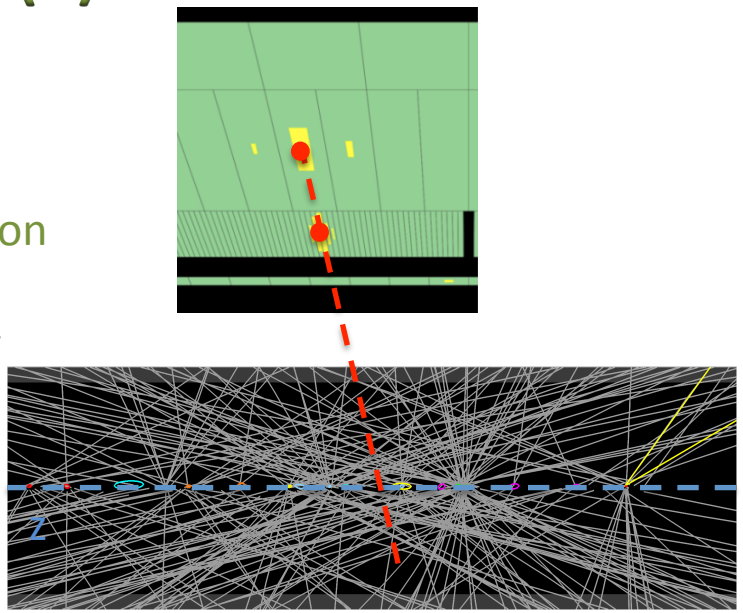

- 4 variables combined in Neural Network (NN) Multi Layer Perceptron
  - $\frac{z_H - z_{vertex}}{\sigma_{vertex}}$ Photon Pointing
  - $\sum p_T^2$ Sum of squared momentum of tracks associated with each vertex
  - $\sum p_T$ Scalar sum of momentum
  - $\Delta\varphi$ between the vertex (defined by the vector sum of the track momenta) and the di-photon system

Efficiency of finding the primary vertex within 0.3 mm of the true one higher than 75%

→ Negligible vertex uncertainty contribution

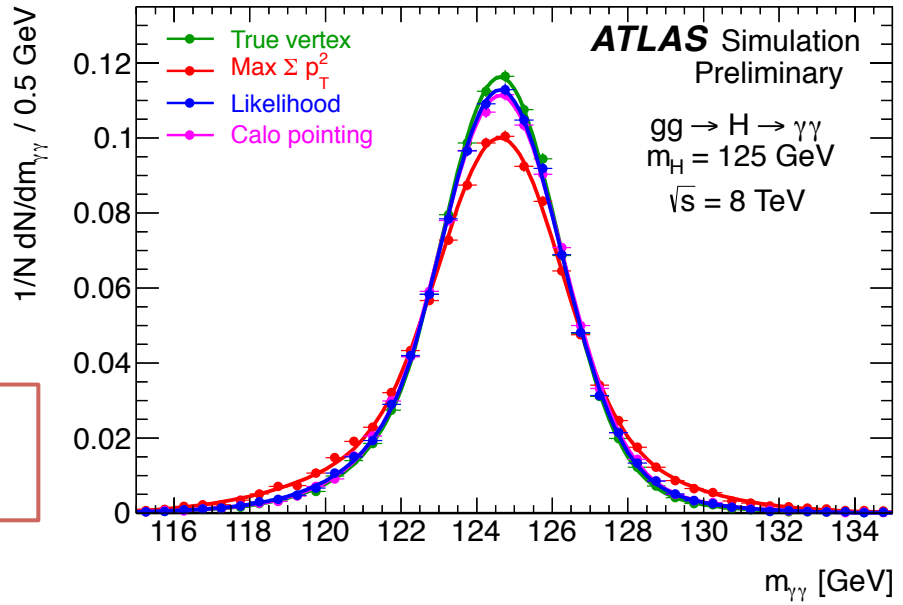

Analysis Categories (1)

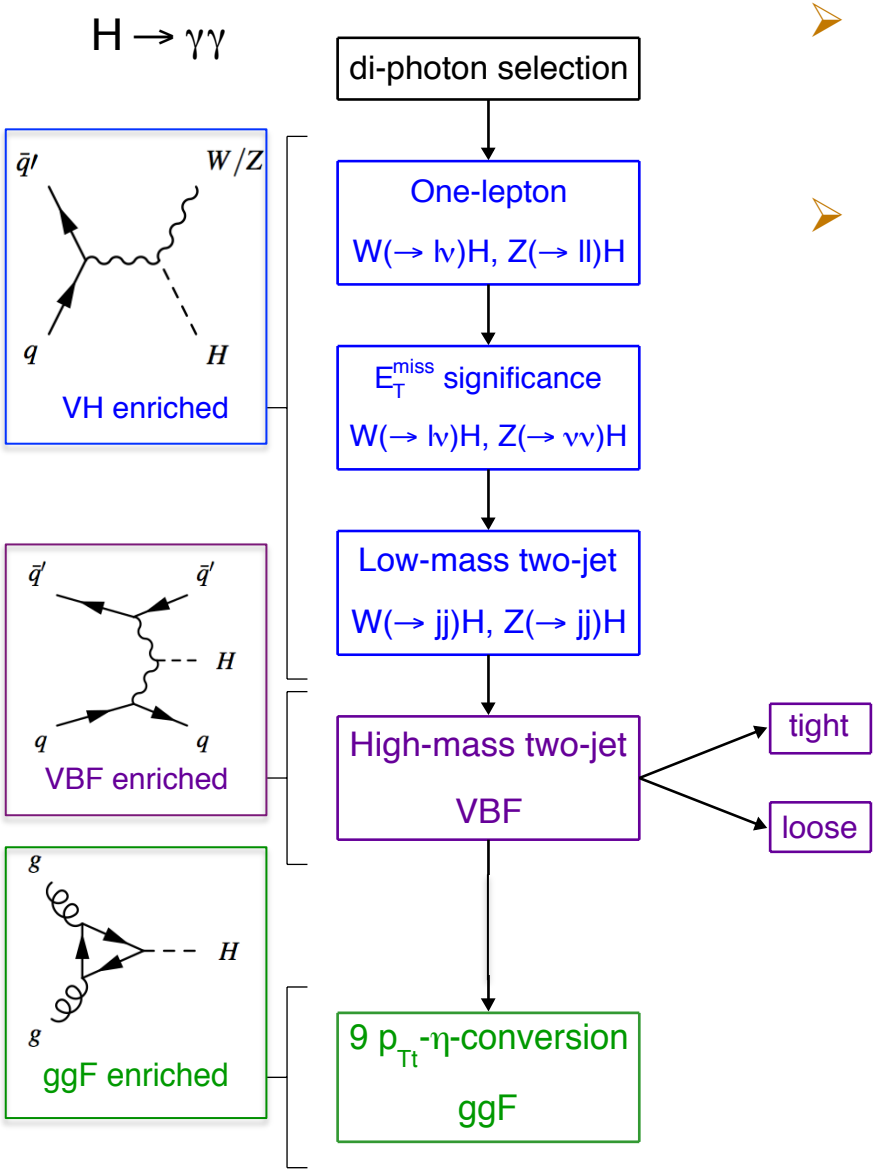

- 14 exclusive categories to increase sensitivity, overall and to specific production processes
- Classify events according to:
  - Production mode:
    - ✓ VH with charged lepton or neutrino tag or V→jj decays
    - ✓ VBF with high mass two jet selection (MVA based)
  - Signal/Background (1-60%) and invariant mass resolution (1.4-2.5 GeV):
    - ✓ p_T of di-photon system
    - ✓ Photon conversion status
    - ✓ Photon impact point in calorimeter

Analysis Categories (2)

14 exclusive categories

$H \rightarrow \gamma\gamma$

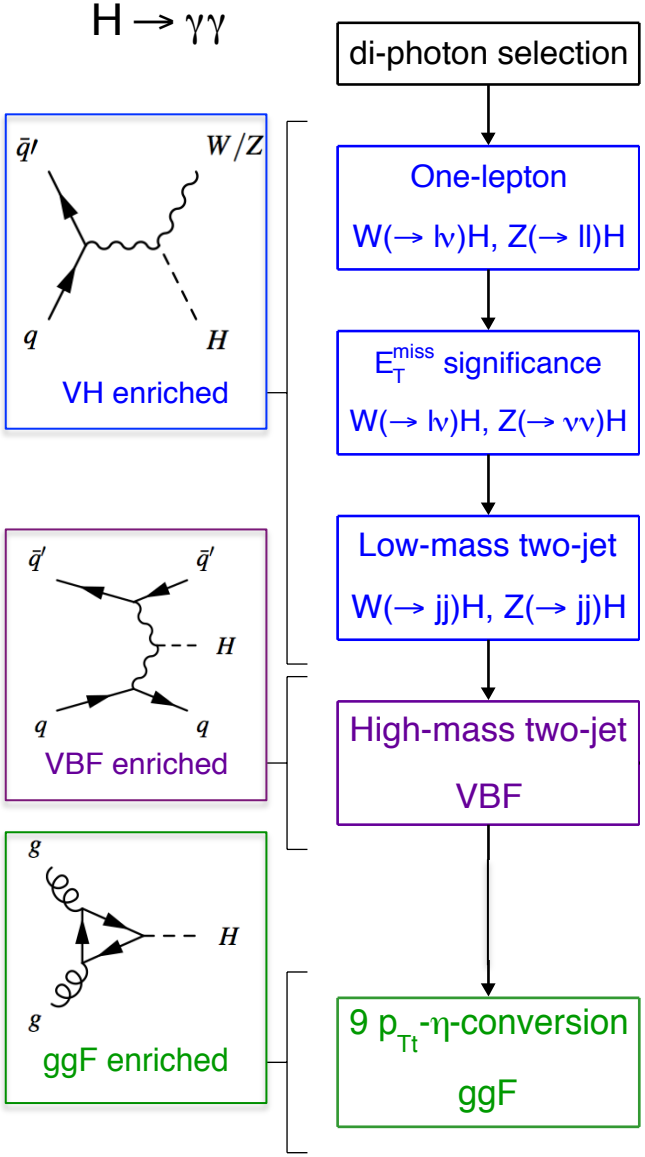

Expected composition of each category:

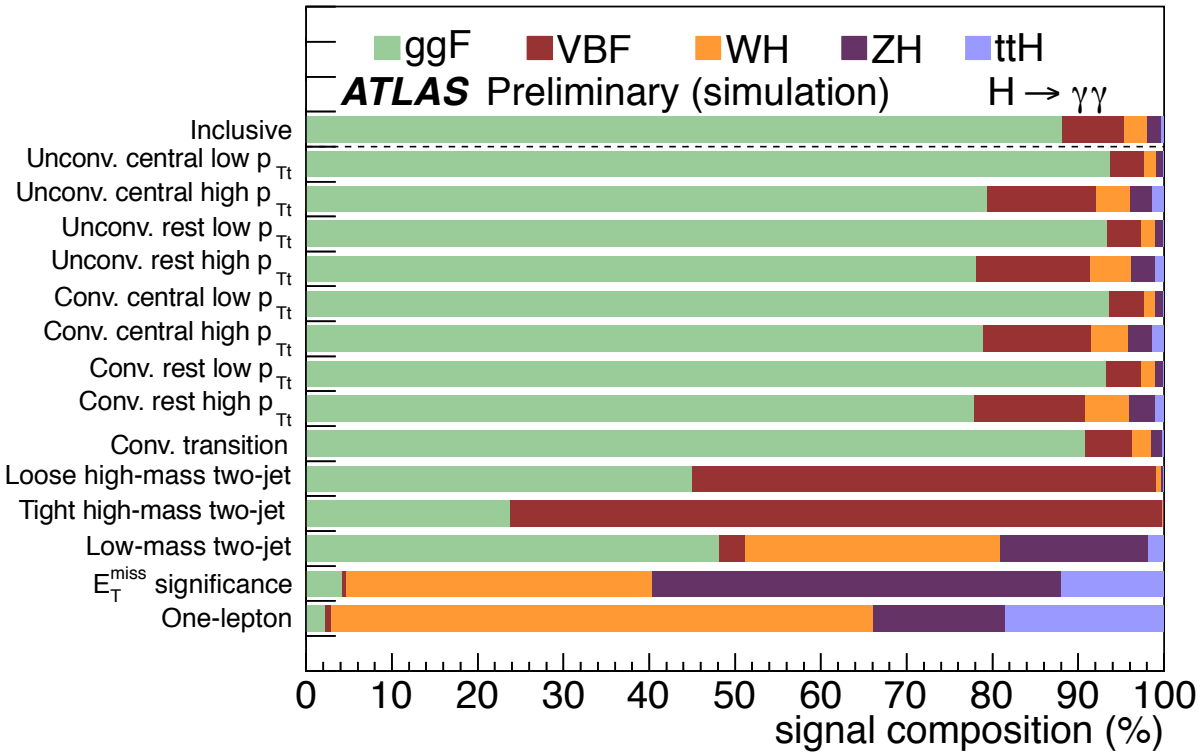

Vector Boson Fusion Selection

- Combination of 8 discriminating variables in a Boosted Decision Tree (BDT) exploiting the VBF topology: 2 forward jets and little hadronic activity between the 2 jets
- BDT trained on VBF signal MC against $\gamma\gamma$ MC (sherpa) and γj+jj from data (non isolated $\gamma\gamma$ sample). Main systematics gluon fusion + jets

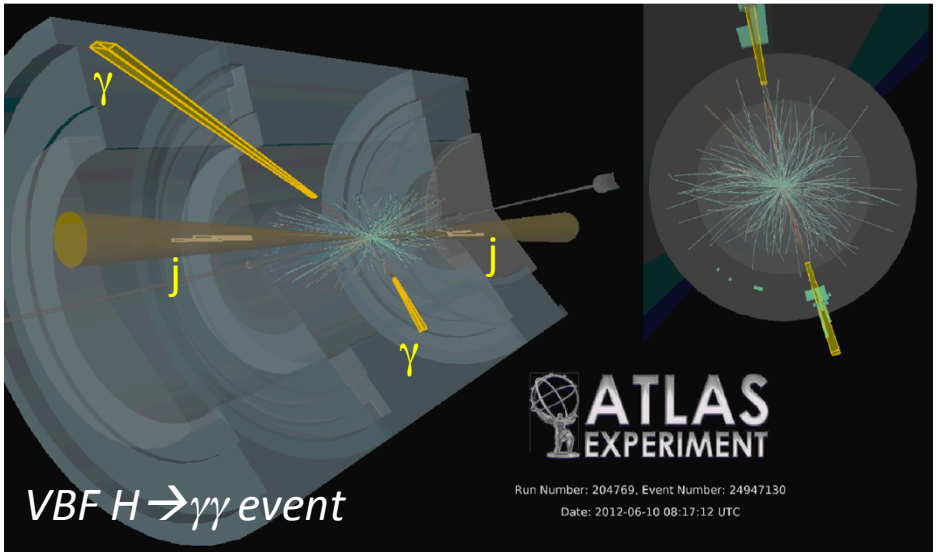

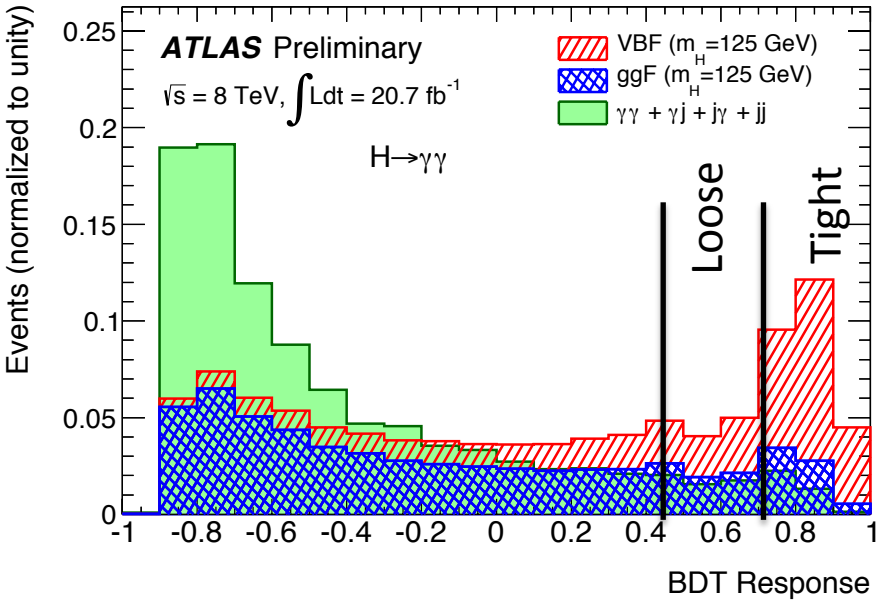

- 2 BDT output categories: loose and tight determined by maximizing the VBF signal significance against ggF and non-resonant backgrounds.

→ Clear separation between the VBF signal and the other processes

Signal Modelling

- The signal is modelled with a Crystal Ball + Gaussian function which is parameterised along the Higgs boson mass

$$N\begin{cases} e^{-t^2/2} & if \quad t > -\alpha_{CB} \\ \left(\frac{n_{CB}}{\alpha_{CB}}\right)^{n_{CB}} e^{-\alpha_{CB}/2} \left(\frac{n_{CB}}{\alpha_{CB}} - \alpha_{CB} - t\right)^{n_{CB}} & otherwise \end{cases}$$

$$t = (m_{\gamma\gamma} - \mu_{CB}) / \sigma_{CB}$$

$$\begin{cases} \mu_{CB}(M) = M + \delta_{\mu} + \Delta_{\mu}(M - 125GeV) \\ \sigma_{CB}(M) = \sigma_{125GeV} + \Delta_{\sigma}(M - 125GeV) \\ \sigma_G = k * \sigma_{CB} \end{cases}$$

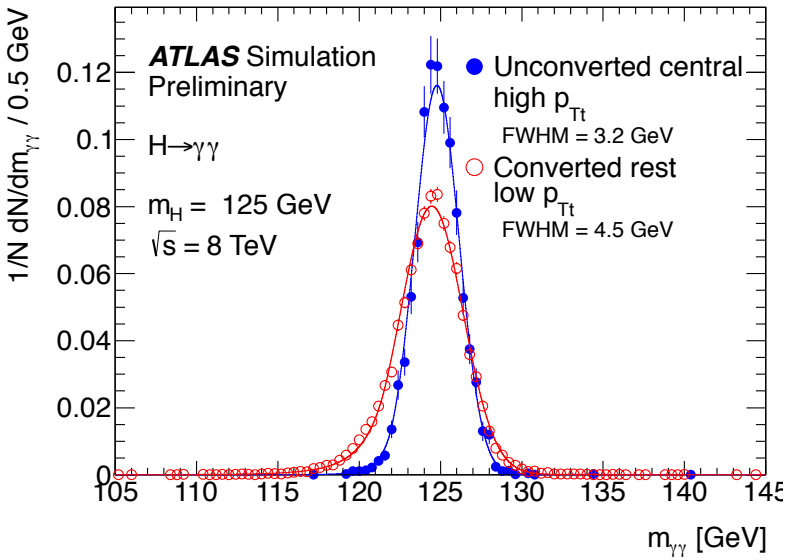

$\sqrt{s}$		8 TeV			
Category	σ_{CB}(GeV)	Observed	N_S	N_B	N_S/N_B
Unconv. central, low p_{Tt}	1.50	911	46.6	881	0.05
Unconv. central, high p_{Tt}	1.40	49	7.1	44	0.16
Unconv. rest, low p_{Tt}	1.74	4611	97.1	4347	0.02
Unconv. rest, high p_{Tt}	1.69	292	14.4	247	0.06
Conv. central, low p_{Tt}	1.68	722	29.8	687	0.04
Conv. central, high p_{Tt}	1.54	39	4.6	31	0.15
Conv. rest, low p_{Tt}	2.01	4865	88.0	4657	0.02
Conv. rest, high p_{Tt}	1.87	276	12.9	266	0.05
Conv. transition	2.52	2554	36.1	2499	0.01
Loose High-mass two-jet	1.71	40	4.8	28	0.17
Tight High-mass two-jet	1.64	24	7.3	13	0.57
Low-mass two-jet	1.62	21	3.0	21	0.14
E_T^{miss} significance	1.74	8	1.1	4	0.24
One-lepton	1.75	19	2.6	12	0.20
Inclusive	1.77	14025	355.5	13280	0.03

Background Modelling

- Analytical function that
  - Minimises the bias (fake signal fitted)
  - Maximises the expected sensitivity (less free parameters)
- The systematic uncertainty = largest signal component over 110-150 GeV from fit on a background only γγ/γj/jj/DY cocktail MC sample

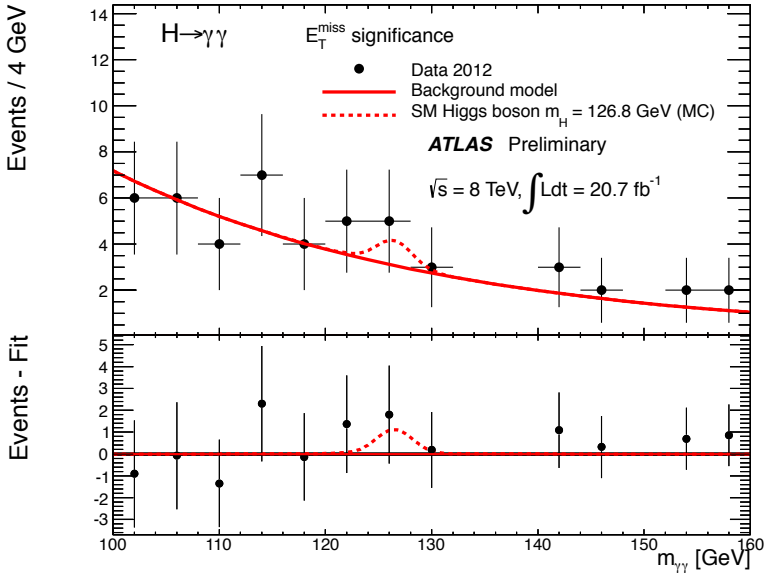

Category	Parametrisation	Uncertainty [N_{evt}] $\sqrt{s}$ = 7 TeV	$\sqrt{s}$ = 8 TeV
Inclusive	4th order pol.	7.3	12.0
Unconverted central, low p_{Tt}	Exp. of 2nd order pol.	2.1	4.6
Unconverted central, high p_{Tt}	Exponential	0.2	0.8
Unconverted rest, low p_{Tt}	4th order pol.	2.2	11.4
Unconverted rest, high p_{Tt}	Exponential	0.5	2.0
Converted central, low p_{Tt}	Exp. of 2nd order pol.	1.6	2.4
Converted central, high p_{Tt}	Exponential	0.3	0.8
Converted rest, low p_{Tt}	4th order pol.	4.6	8.0
Converted rest, high p_{Tt}	Exponential	0.5	1.1
Converted transition	Exp. of 2nd order pol.	3.2	9.1
Loose high-mass two-jet	Exponential	0.4	1.1
Tight high-mass two-jet	Exponential	-	0.3
Low-mass two-jet	Exponential	-	0.6
E_T^{miss} significance	Exponential	-	0.1
One-lepton	Exponential	-	0.3

For very low statistics categories, inclusive uncertainty is scaled to statistics

→ The systematics is then treated as a spurious term in the signal

Systematic Uncertainties Main Sources

Uncertainties on the signal yield

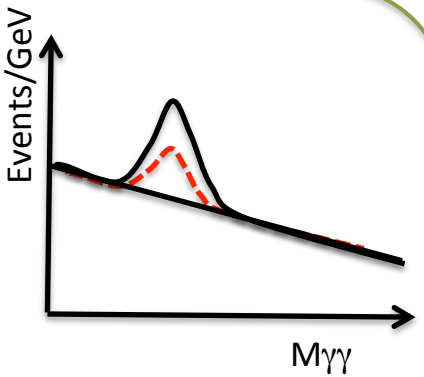

Theory: Branching ratio, scale, PDF, cross section (˜12% overall, up to 50% for 2-jets)
Luminosity (1.8-3.6%), Photon identification efficiency (2.4%), Background model (˜3%)

Uncertainties on the signal resolution

More later

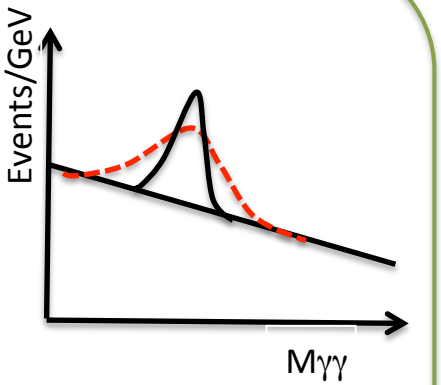

Calorimeter energy resolution extrapolation from Z→ee events (14-23% along categories)

Uncertainties on the migrations between categories

Jet energy scale (up to 20%)
Underlying events (up to 13%)
Higgs p_{Tt} modelling (up to 10%)
Material mis-modelling (˜4%)

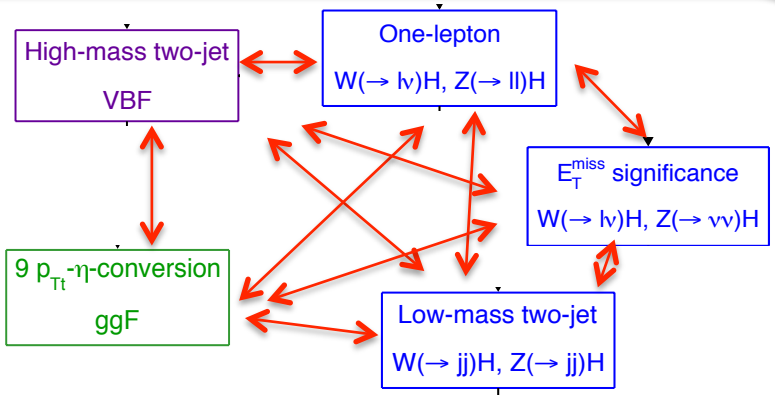

Results

- Invariant mass distribution, overlaid background + signal fit

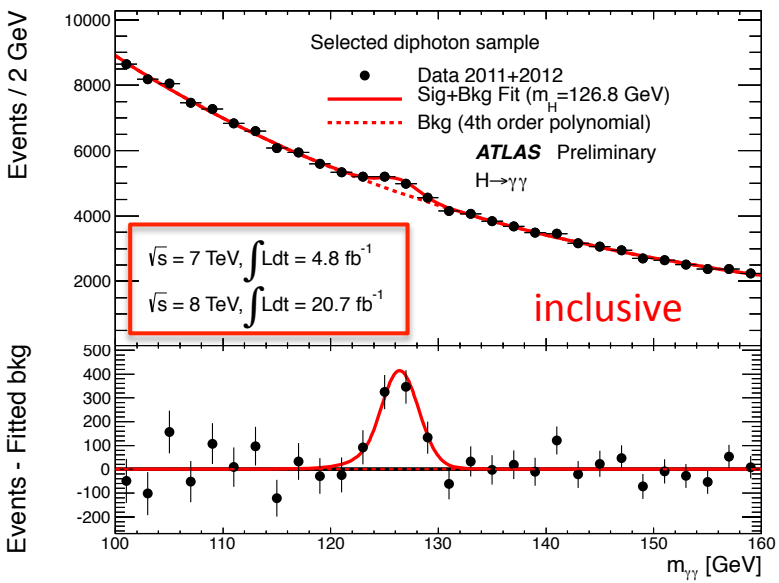

Effect of categories

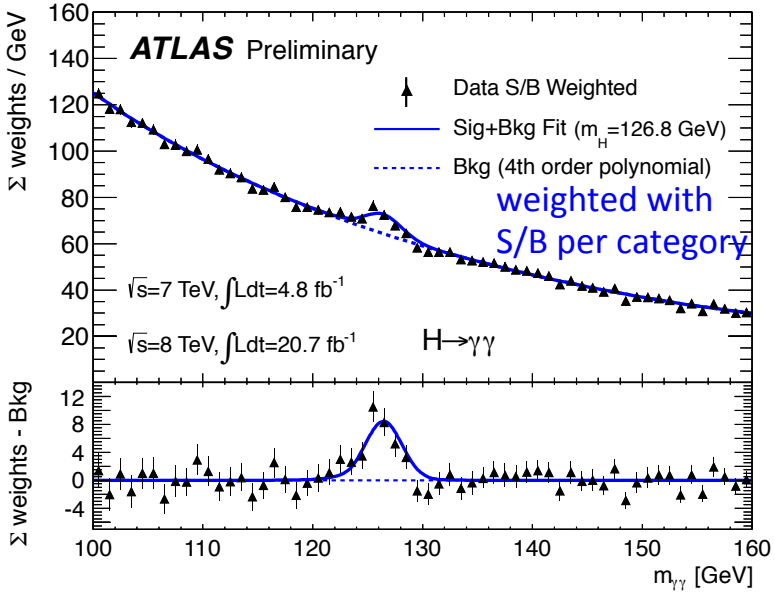

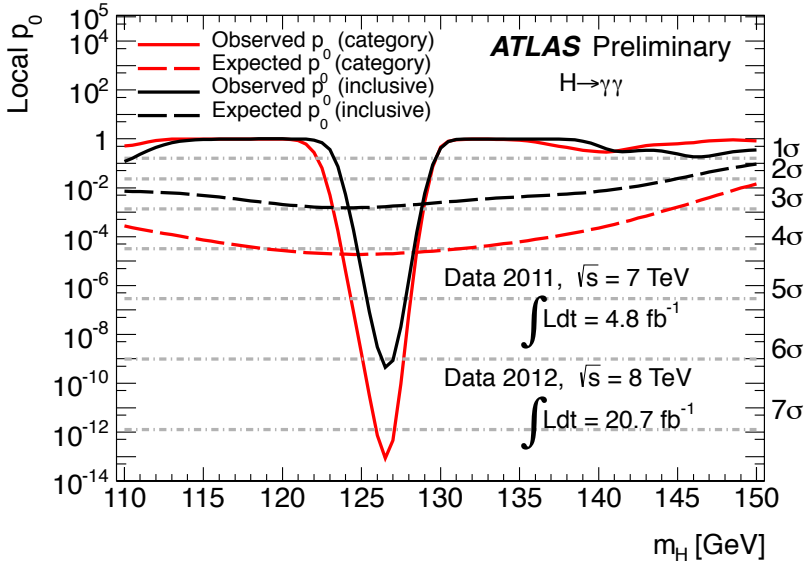

- Observed local significance of the excess: 7.4 σ for 4.3 σ expected (at $M_{\gamma\gamma}$ = 126.5 GeV)
- Best mass fit: 126.8 ± 0.2 (stat) ± 0.7 (syst) GeV
- Best fit of signal strength at this mass:

  $\mu = \sigma/\sigma_{SM} = 1.57 \pm 0.22(\text{stat})\ ^{+0.24}(\text{syst})$
- Inclusive fiducial cross section of observed particle: $\sigma_{fid}.BR = 56.2 \pm 12.5$ fb

Signal Strength Combination

- Combination of bosonic decays (WW, ZZ, γγ):
  μ =1.33±0.21
- Signal strengths in fermionic decay modes have large uncertainties, but are compatible with SM value of 1
- Including H→ττ and H→bb results:
  μ = 1.23 ± 0.18

→ Data are consistent with the hypothesis of a Standard Model Higgs boson.

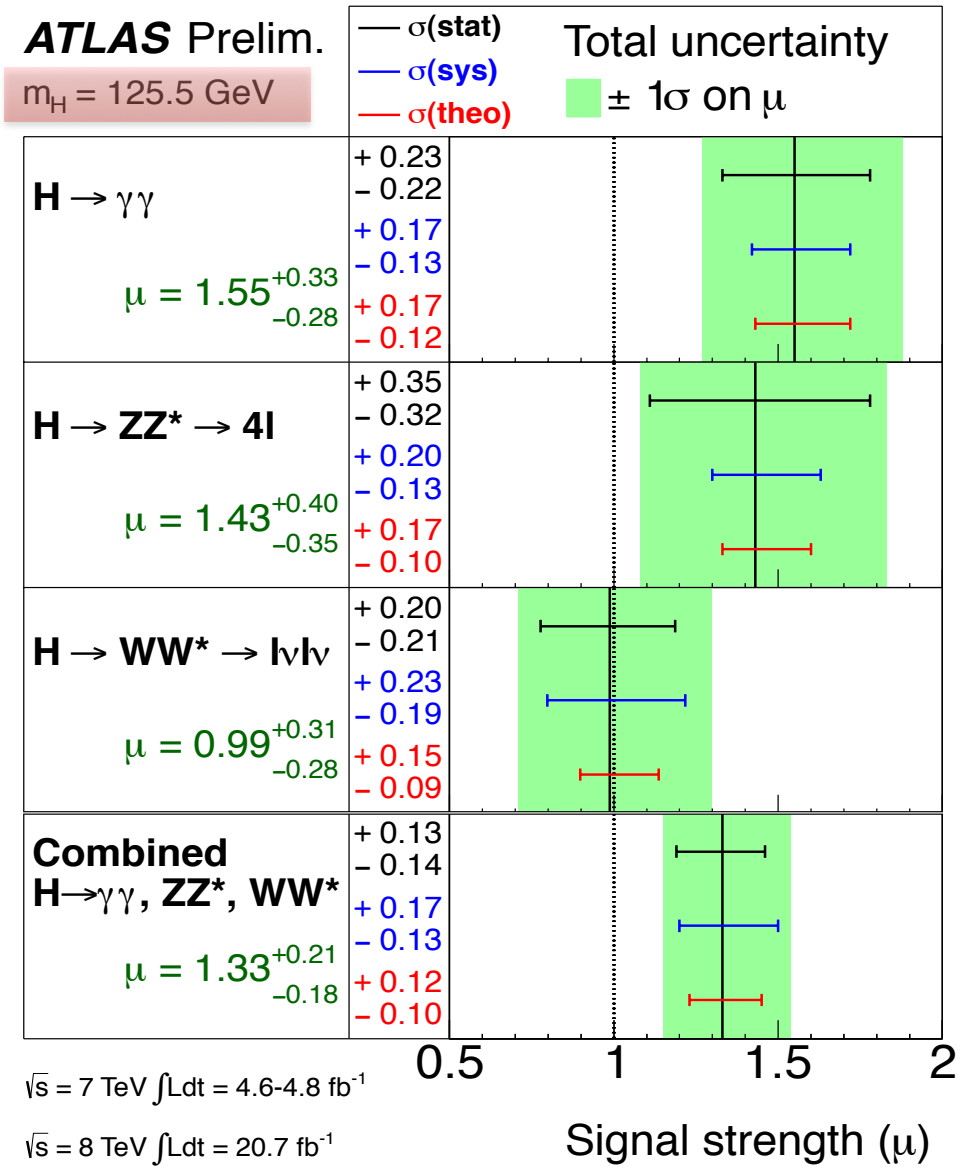

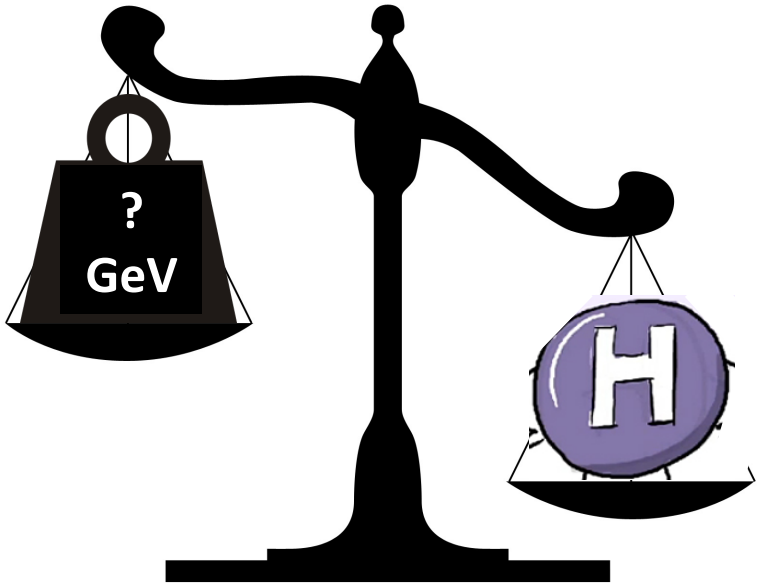

MASS DETERMINATION

An Interesting Mass

- A Higgs boson mass around 125 GeV is interesting in 2 ways:
  - Theoretically:

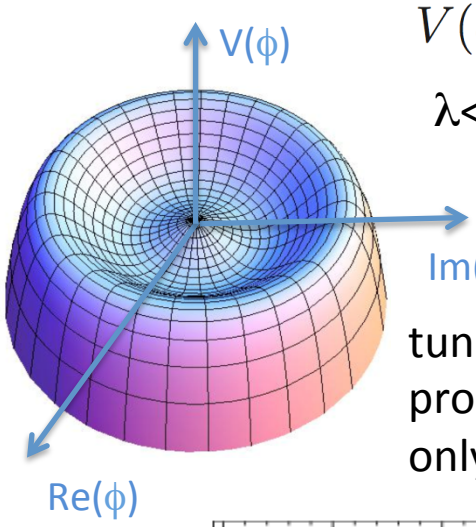

$$V(\phi) = \mu^2 \mid \phi \mid^2 + \lambda \mid \phi \mid^4$$

λ<0: meta-stability region

tunnelling probability proportional to $e^{1/\lambda}$, and λ is only slightly negative

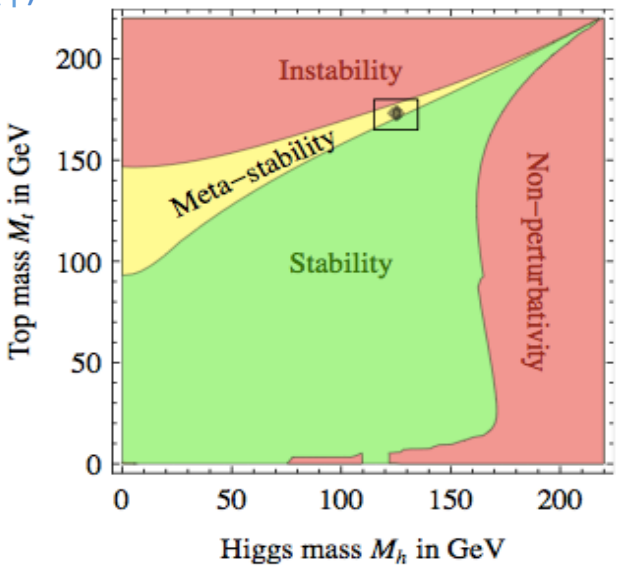

  - Experimentally:

Observable in many channels, great potential for couplings measurement (κ_{top}, κ_b, κ_V (W,Z), κ_τ, κ_μ, κ_γ, κ_{gluons})

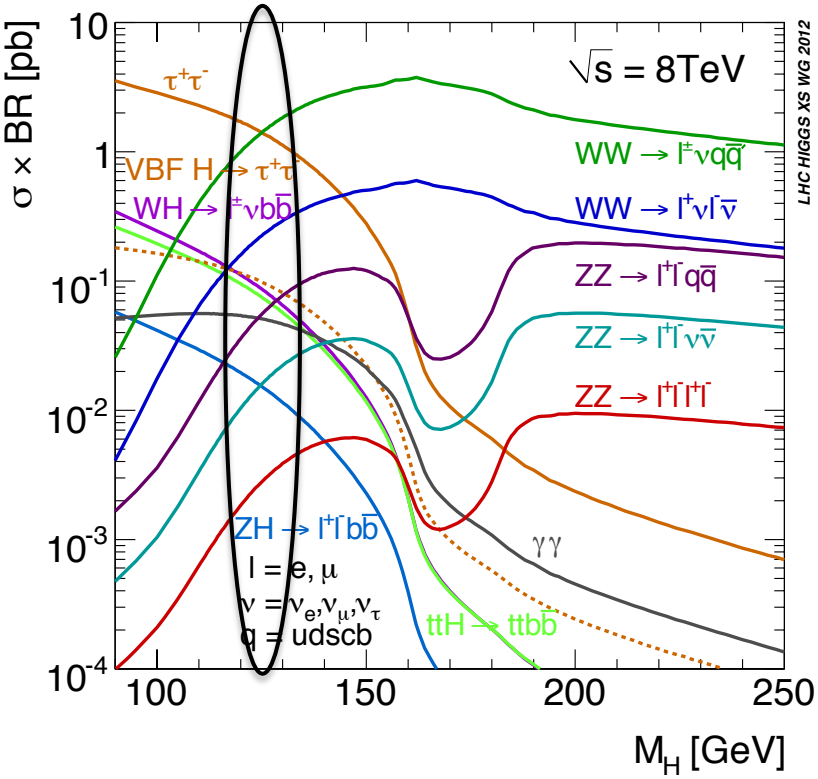

Uncertainties on Boson Mass for H→γγ channel

Energy scale from
Z → ee (0.3%)

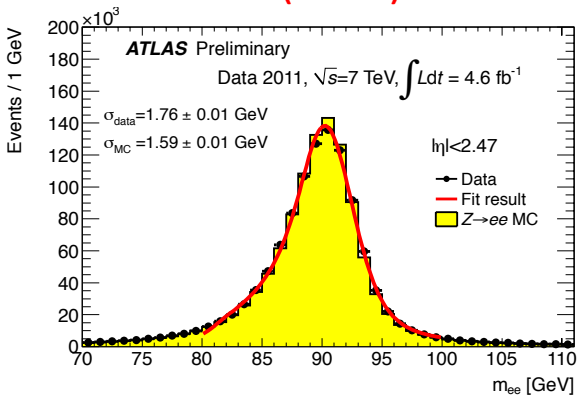

Upstream material
simulation (0.3%)

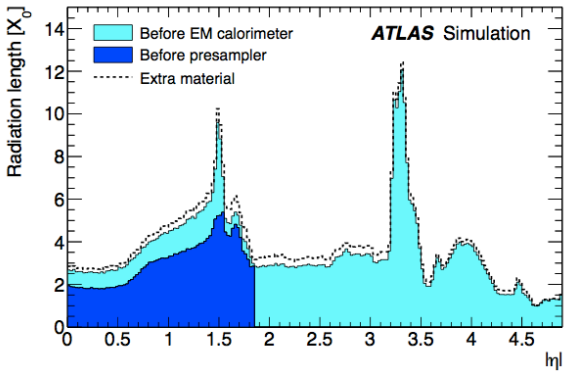

Conversion fraction 0.1%

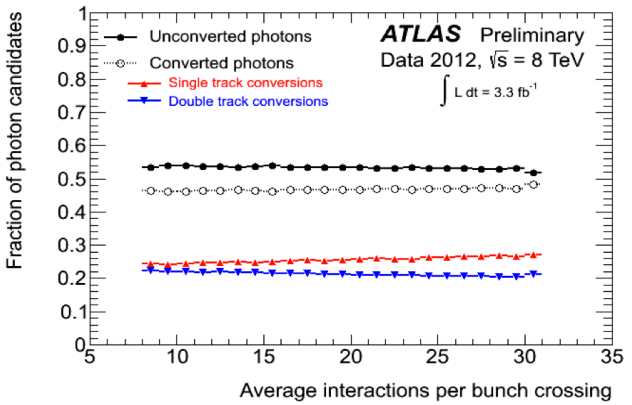

Pre-sampler energy scale (0.1%)

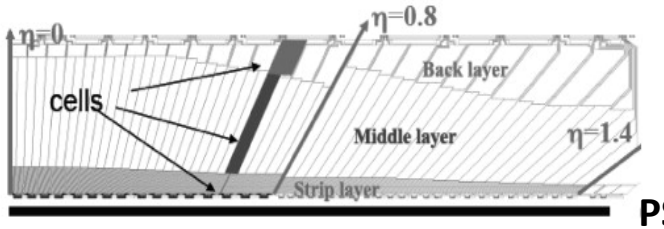

Relative calibration of 1st and 2nd sampling 0.2%

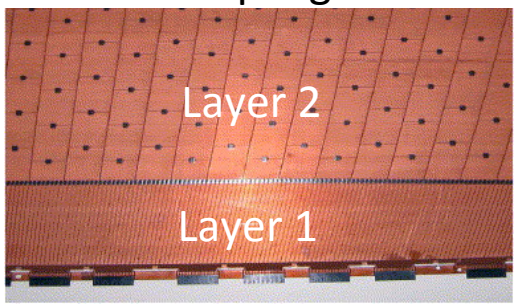

Non-linearities of the EM calorimeter electronics 0.15%

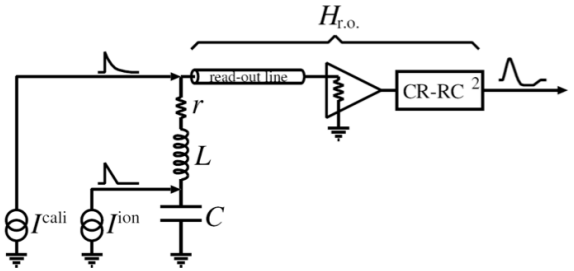

Lateral leakage corrections 0.1%

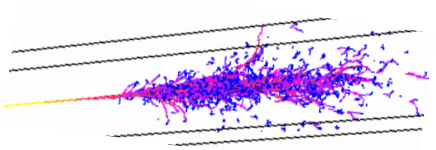

+ other smaller effects

→ Total uncertainty: 0.55% (0.7 GeV)

γγ mass measurements with different photon energy calibration (η & p_T categories), conversion status and pile-up conditions give consistent results

γγ and ZZ Mass Compatibility

- γγ and ZZ final states both high resolution and are optimal for mass determination

  (ZZ systematics uncertainty determined with J/Ψ→ll, Υ→μμ and Z→ll decays)

$H\to\gamma\gamma$: $M_H = 126.8 \pm 0.2(\text{stat}) \pm 0.7(\text{sys})$ GeV

$H\to ZZ(*)\to 4l$: $M_H = 124.3 \pm 0.6\ (\text{stat})\ ^{+0.5}_{-0.3}\ (\text{sys})$ GeV

Combination: $M_H = 125.5 \pm 0.2\ (\text{stat})\ ^{+0.5}_{-0.6}\ (\text{sys})$ GeV

(CMS: 125.7±0.3(stat.)±0.3(syst.) GeV)

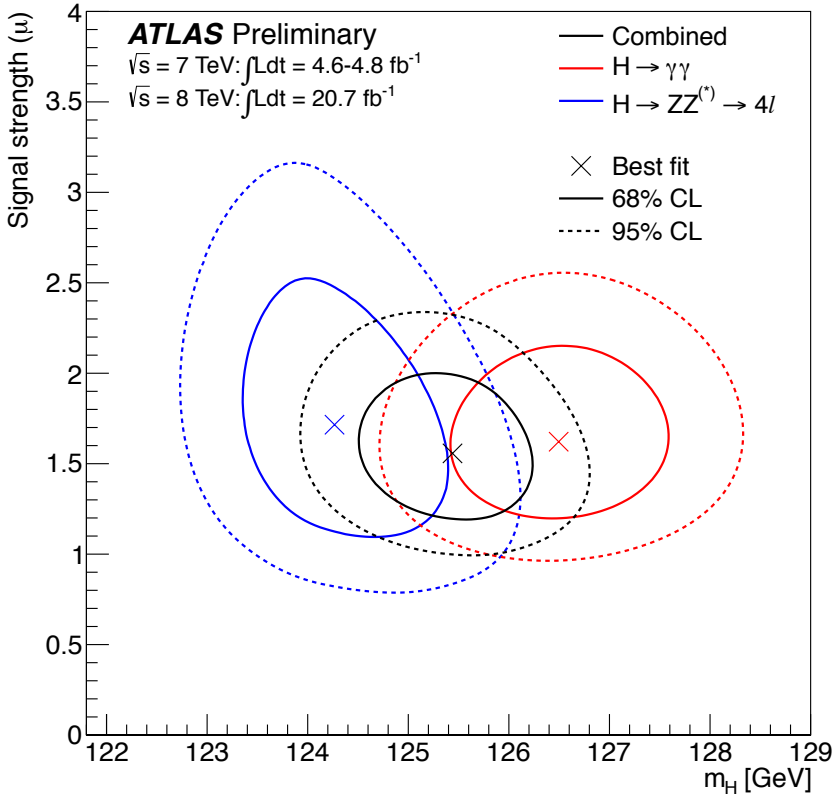

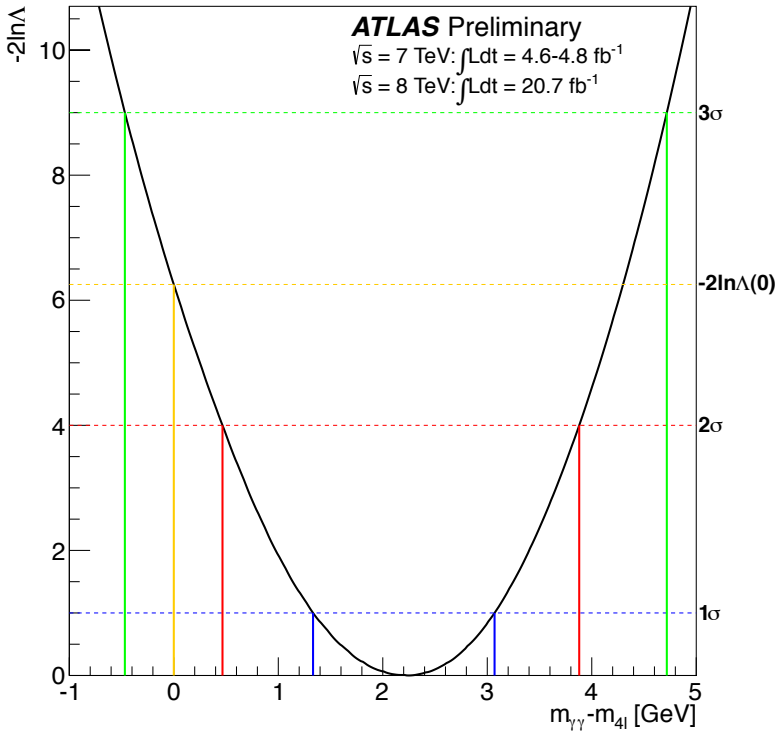

Fitted mass discrepancy:

$\Delta m_H = m_H^{\gamma\gamma} - m_H^{4l} = 2.3 \pm 0.6(\text{stat}) \pm 0.6\ (\text{syst})$ GeV

Probability for such mass disagreement or higher using MC pseudo experiments is 1.5% or 2.4σ

Is the observed boson the the Standard Model Higgs ?

COUPLINGS AND SPIN MEASUREMENTS

First look at the couplings

- Production mechanisms associated with either top (ggF+ttH) or gauge bosons (VBF +VH) couplings: agreement with the Standard Model at the 2σ level for γγ

Gauge bosons coupling

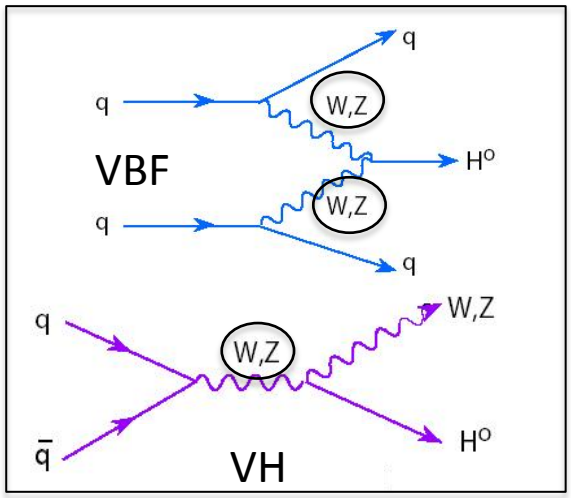

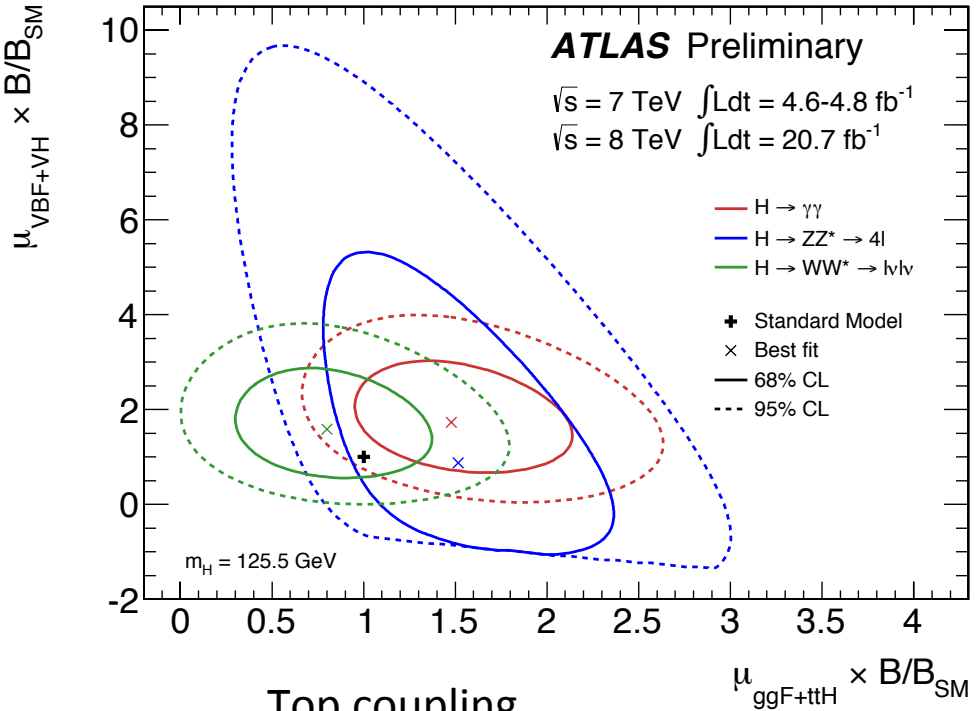

Top coupling

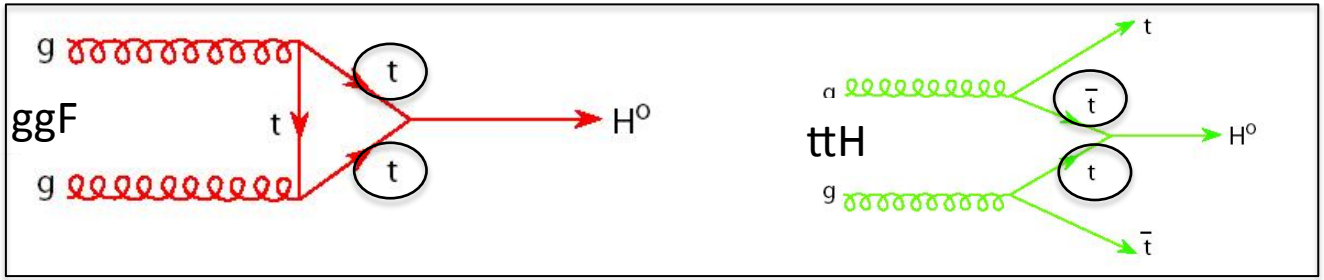

Further Split for H→γγ Couplings

- Further split of VBF and VH production:
  - Improvements wrt to previous analysis thanks to additional VH categories and VB MVA categories

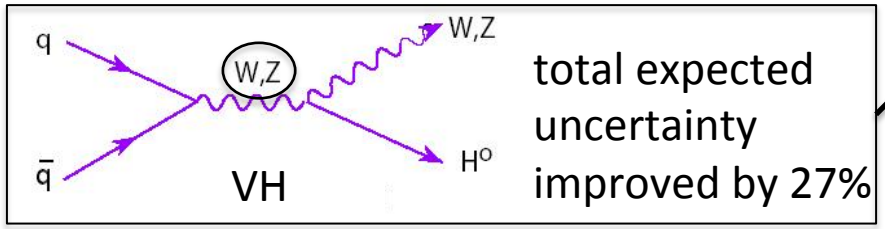

total expected uncertainty improved by 27%

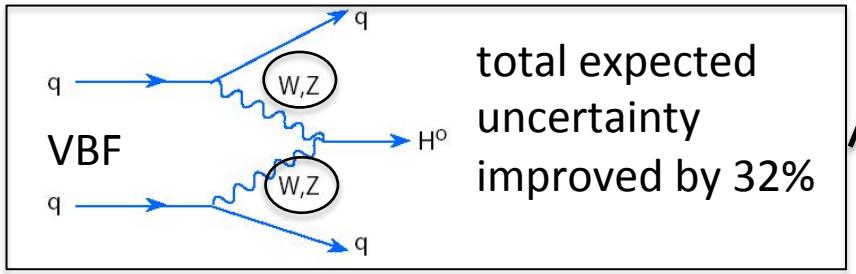

total expected uncertainty improved by 32%

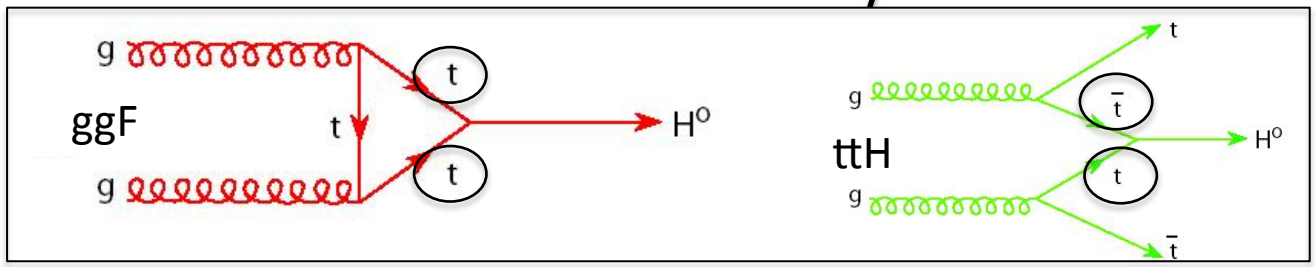

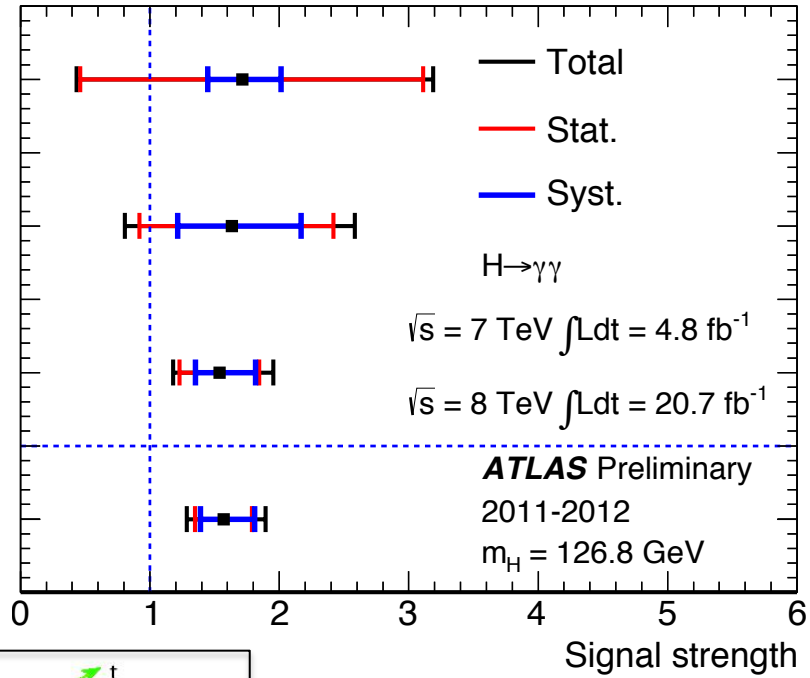

→ Signal strength per production process all compatible with each other

H→ γγ Spin Analysis Model

- Higgs boson candidate observed in the di-photon channel: Landau-Yang theorem excludes spin 1 hypothesis → only spin-2 hypothesis tested
- The most general interaction of a spin-2 particle with gauge boson pair has 10 independent effective couplings constants ($g_{1,\ldots,10}$)
  - Considering available statistics, a $J^P = 2_m^+$ graviton-like minimal couplings model is considered
    - ✓ The only dependencies are the coupling intensities to the SM fields (g_1=g_5=1)

$$A(X \to VV) = \Lambda^{-1} \left[2g_1^{(2)} t_{\mu\nu} f^{*1,\mu\alpha} f^{*2,\nu\alpha} + 2g_2^{(2)} t_{\mu\nu} \frac{q_\alpha q_\beta}{\Lambda^2} f^{*1,\mu\alpha} f^{*2,\nu,\beta} \right.$$
$$+ g_3^{(2)} \frac{\tilde{q}^\beta \tilde{q}^\alpha}{\Lambda^2} t_{\beta\nu} (f^{*1,\mu\nu} f^{*2}_{\mu\alpha} + f^{*2,\mu\nu} f^{*1}_{\mu\alpha}) + g_4^{(2)} \frac{\tilde{q}^\nu \tilde{q}^\mu}{\Lambda^2} t_{\mu\nu} f^{*1,\alpha\beta} f^{*(2)}_{\alpha\beta}$$
$$+ m_V^2 \left(2g_5^{(2)} t_{\mu\nu} \epsilon_1^{*\mu} \epsilon_2^{*\nu} + 2g_6^{(2)} \frac{\tilde{q}^\mu q_\alpha}{\Lambda^2} t_{\mu\nu} (\epsilon_1^{*\nu} \epsilon_2^{*\alpha} - \epsilon_1^{*\alpha} \epsilon_2^{*\nu}) + g_7^{(2)} \frac{\tilde{q}^\mu \tilde{q}^\nu}{\Lambda^2} t_{\mu\nu} \epsilon_1^* \epsilon_2^* \right)$$
$$\left. + g_8^{(2)} \frac{\tilde{q}_\mu \tilde{q}_\nu}{\Lambda^2} t_{\mu\nu} f^{*1,\alpha\beta} \tilde{f}^{*(2)}_{\alpha\beta} + g_9^{(2)} t_{\mu\alpha} \tilde{q}^\alpha \epsilon_{\mu\nu\rho\sigma} \epsilon_1^{*\nu} \epsilon_2^{*\rho} q^\sigma + \frac{g_{10}^{(2)} t_{\mu\alpha} \tilde{q}^\alpha}{\Lambda^2} \epsilon_{\mu\nu\rho\sigma} q^\rho \tilde{q}^\sigma \, (\epsilon_1^{*\nu} (q\epsilon_2^*) + \epsilon_2^{*\nu} (q\epsilon_1^*)) \right]$$

  - H→γγ has low sensitivity to parity (more easily determined by H→ZZ)
    - ✓ No comparison to CP-odd model

H→ γγ Spin Discriminating Variable

- Discriminating variable cosθ*, polar angle of photons wrt the z axis in the Collins-Soper frame (z axis along bisector of beam direction)

$$\cos\theta^* = \frac{\sinh(\eta_{\gamma_1} - \eta_{\gamma_2})}{\sqrt{1 + \left(p_{\mathrm{T}}^{\gamma\gamma}/m_{\gamma\gamma}\right)^2}} \cdot \frac{2 p_{\mathrm{T}}^{\gamma_1} p_{\mathrm{T}}^{\gamma_2}}{m_{\gamma\gamma}^2}$$

  - In principle least sensitive to ISR
  - shown also to be the most discriminant between spin0 and spin2

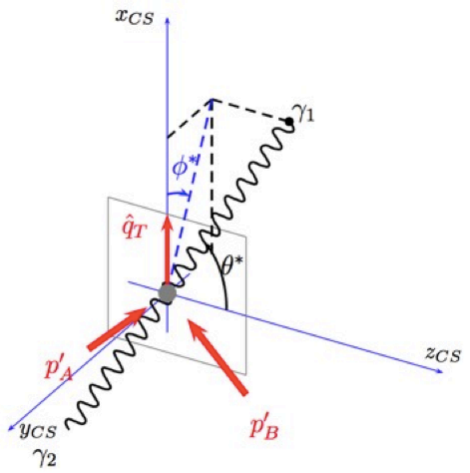

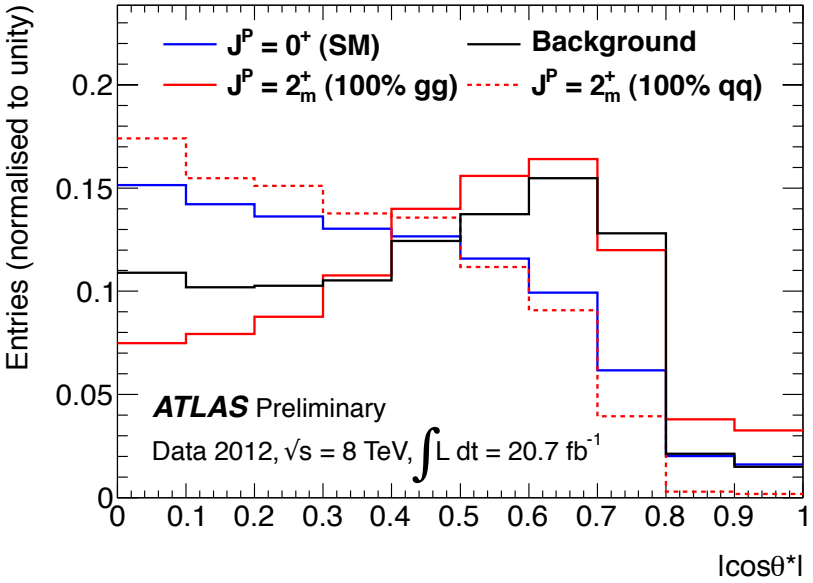

- Compare the dN/dcosθ* distribution:
  - Flat for H→γγ before acceptance & kinematic cuts
  - ~ 1 + 6 $\cos^2\theta^*$ + $\cos^4\theta^*$ for gg initiated spin 2
  - ~ 1 – $\cos^4\theta^*$ for qq initiated spin 2

  (from Wigner matrices and helicity formalism)
- Good discrimination for gluon fusion, worse for qq initial state

H→ γγ Spin Properties

- Fit the data for the 2 hypotheses: SM $J^P = 0^+$ and $J^P = 2_m^+$ assuming no correlation between $\cos\theta^*$ and $m_{\gamma\gamma}$ in the signal region

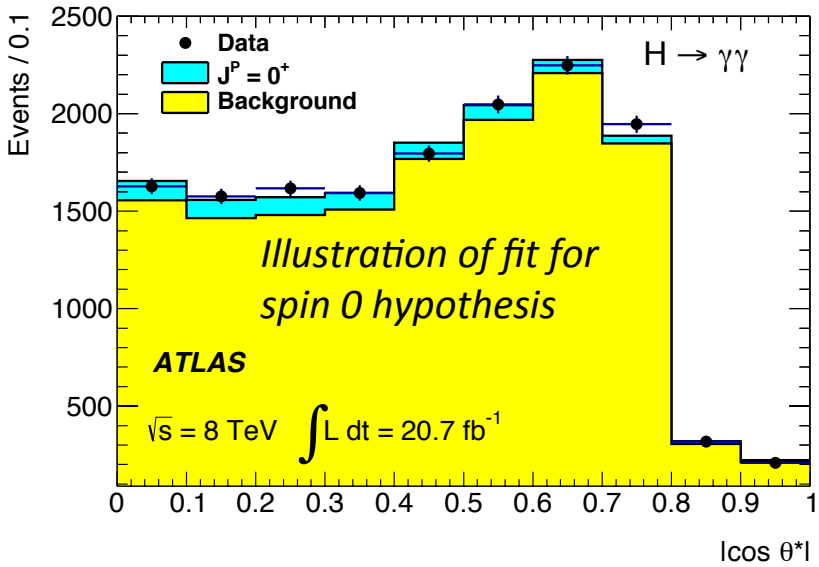

Background subtraction

conditional fit with different spin 0 $\cos\theta^*$ shape

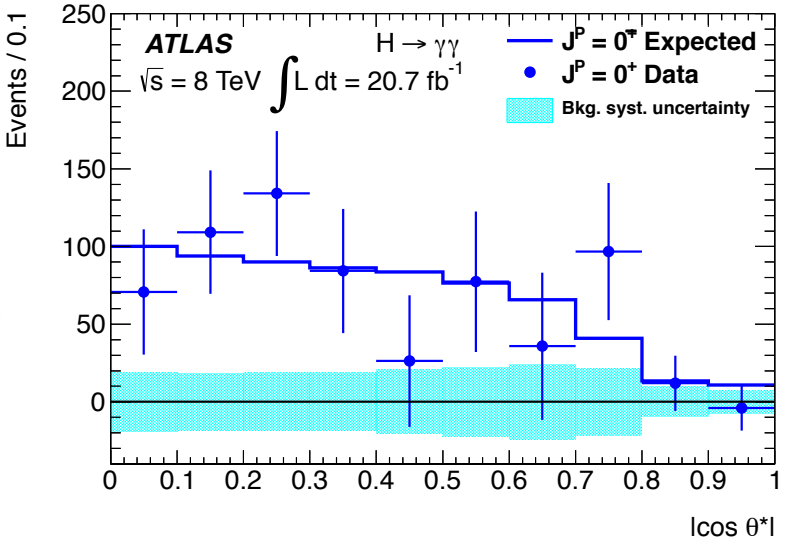

- Test statistics is likelihood ratio between SM and spin 2

$$q = \ln \frac{\mathcal{L}_0(\hat{\hat{\theta}}_0)}{\mathcal{L}_2(\hat{\hat{\theta}}_2)}$$

- Spin 2 hypothesis excluded at 99.3% CL if 100% gluon fusion
- Sensitivity maximum at high fraction of ggF, degraded for higher fractions of qq → complementarity with WW channel

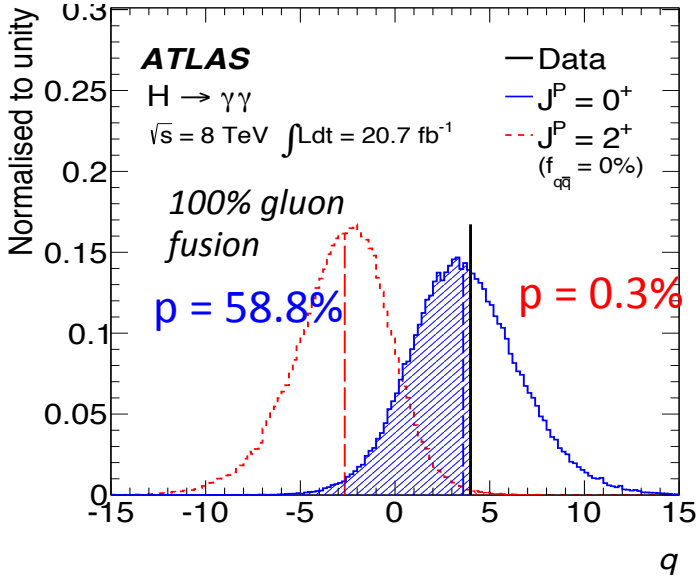

Spin Combination

- Standard Model spin $JP=0^+$ is favoured compared to:
  - $JP=0^-$ (ZZ)
  - $JP=1^{+/-}$ (ZZ and WW)
  - $JP=2_m^+$ ($\gamma\gamma$, ZZ and WW)

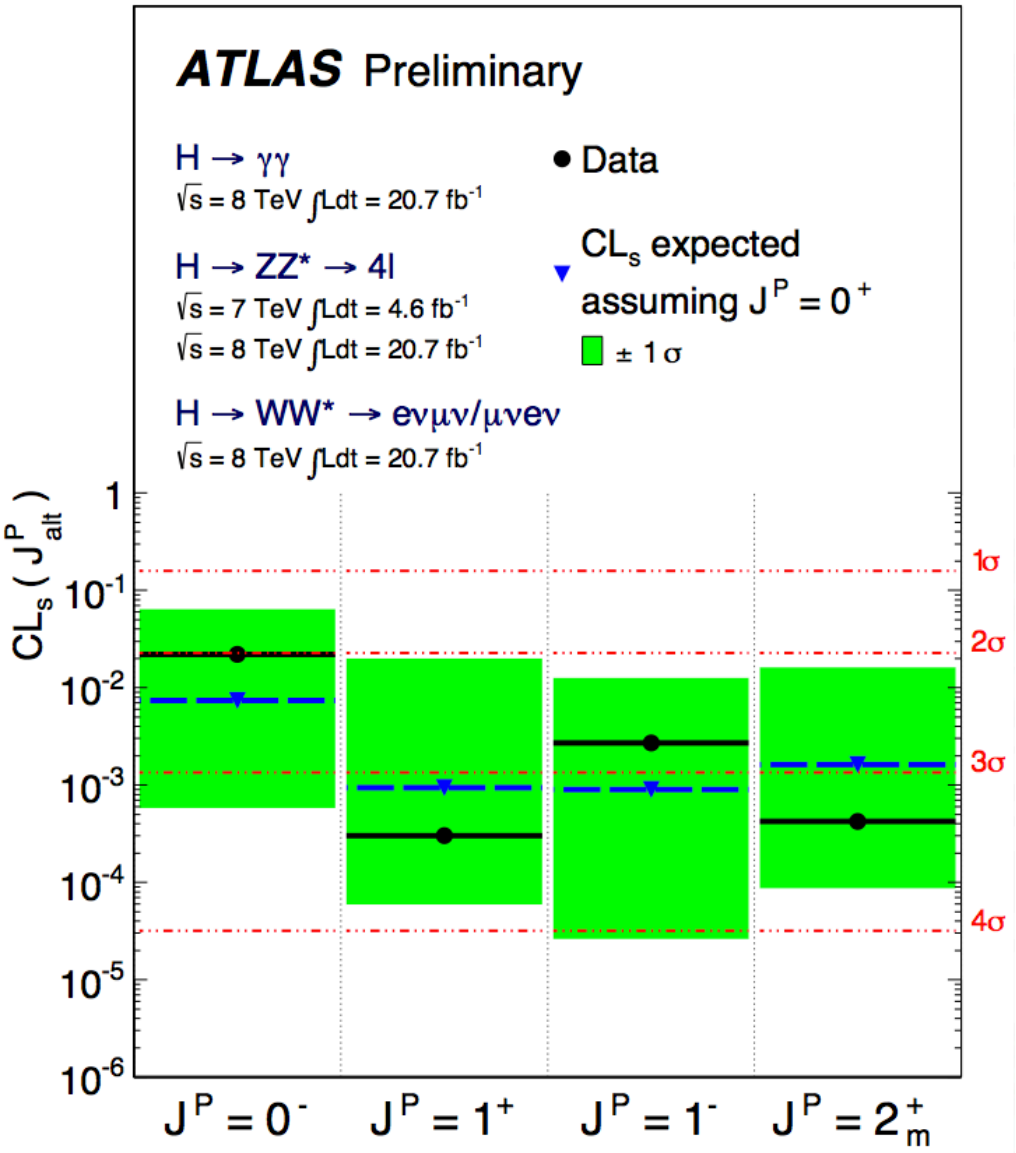

PROSPECTS

Detector and Performance Prospects

2013-2015		2018-2019		2021-2023	
~25 fb^{-1} @ 7-8 TeV $6x10^{33}cm^{-2}s^{-1}$ <μ>=20 (50 ns)	0	≥ 50 fb^{-1} @ 13-14 TeV $10^{34}cm^{-2}s^{-1}$ <μ>=27 (25 ns)	Phase I	≥ 300 fb^{-1} $2\text{-}3x10^{34}cm^{-2}s^{-1}$ <μ>=55	II	~3000 fb^{-1} <μ>=140

- Improvement of performance

Main handle for H→γγ systematics reduction: Photon energy scale

- Extrapolation from Z→e^+e^- electrons to photons
  - ✓ More studies of the upstream material
- Direct study of radiative photons Z→eeγ et Z→μμγ

+ Multivariate techniques for calibration

- Phase II: replacement of the read out electronics

- Detector upgrade for higher luminosities:

Level 1 trigger towers
$\Delta\eta x\Delta\phi=0.1x0.1$

Super-cells
$\Delta\eta x\Delta\phi=0.025x0.1$ (S1 & S2)
$\Delta\eta x\Delta\phi=0.1x0.1$ (PS & S3)

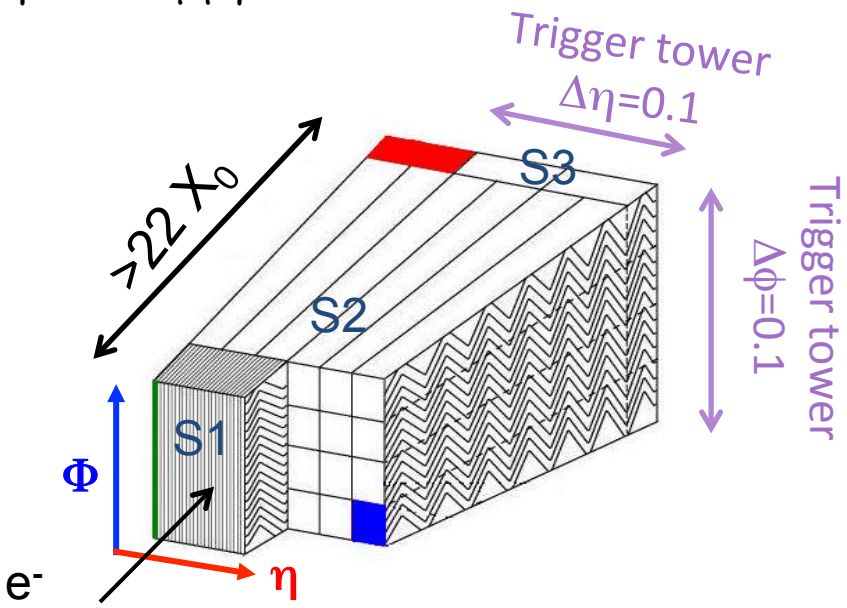

→ Keep trigger at low p_T for EM objects

Physics Measurements Prospects

2013-2015 | 2018-2019 | 2021-2023

~25 fb^{-1} @ 7-8 TeV, 6x10^{33}cm^{-2}s^{-1} → 0 → ≥ 50 fb^{-1} @ 13-14 TeV, 10^{34}cm^{-2}s^{-1} → Phase I → ≥ 300 fb^{-1}, 2-3x10^{34}cm^{-2}s^{-1} → II → ~3000 fb^{-1}

- Determination of the Higgs couplings

κ_V (bosons) : ±10% ⇢ ±3-6%

κ_F (fermions) : ±25% ⇢ ±2-4%

$$\kappa_X^2 = \frac{\Gamma_{H\to X}}{\Gamma_{H\to X}^{SM}}$$

κ_{top}, κ_b, κ_V (W,Z), κ_τ, κ_μ, κ_γ, κ_{gluons} + Higgs self-coupling

±20-50% ⇢ ±5-25%

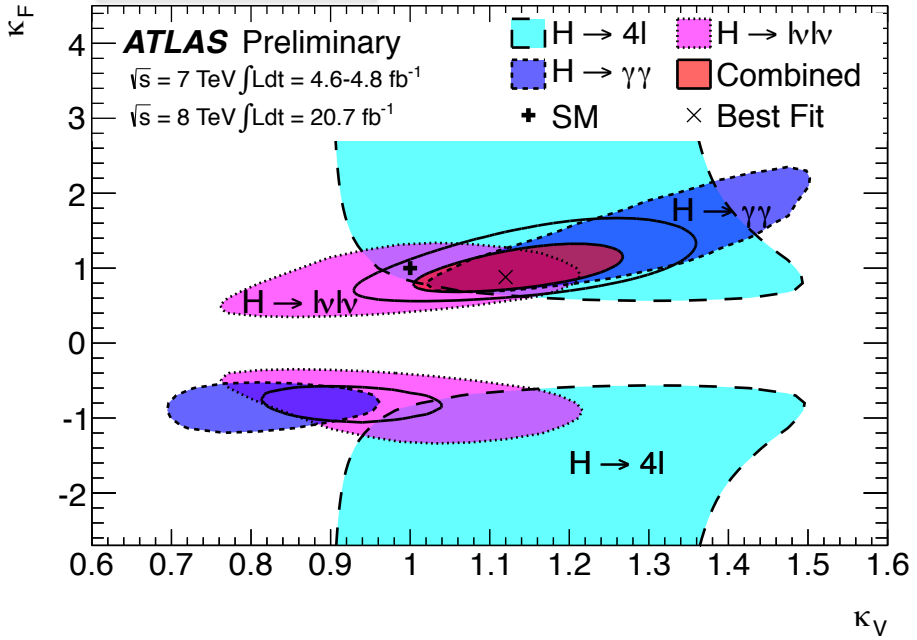

→ New physics through evidence of couplings deviation from Standard Model

- Coupling to other scalars (Minimal Super-Symmetric Models)
- Decays to non observed final states (invisible channels)
- Loops in production diagrams modified by presence of new virtual particles
- Boson not an elementary particle

Conclusions

- With the present uncertainties, ATLAS data are consistent with the expectations for the Standard Model Higgs boson
  - Production rates and coupling strengths, evidence for VBF production
  - Other spins tested (0^-, 1^+, 1^-, 2^+_m) disfavoured compared to SM 0^+

- The di-photon channel, with clear signature, high background rejection and high mass resolution contributed greatly to this achievement
  - Significant signal significance (7.4σ) which excludes spin-1 hypothesis (Landau Yang)
  - Signal strengths compatible for various Higgs boson production modes (VH, VBF, ggF+ttH)
  - Spin-2 graviton-like minimal coupling model disfavoured compared to SM 0^+

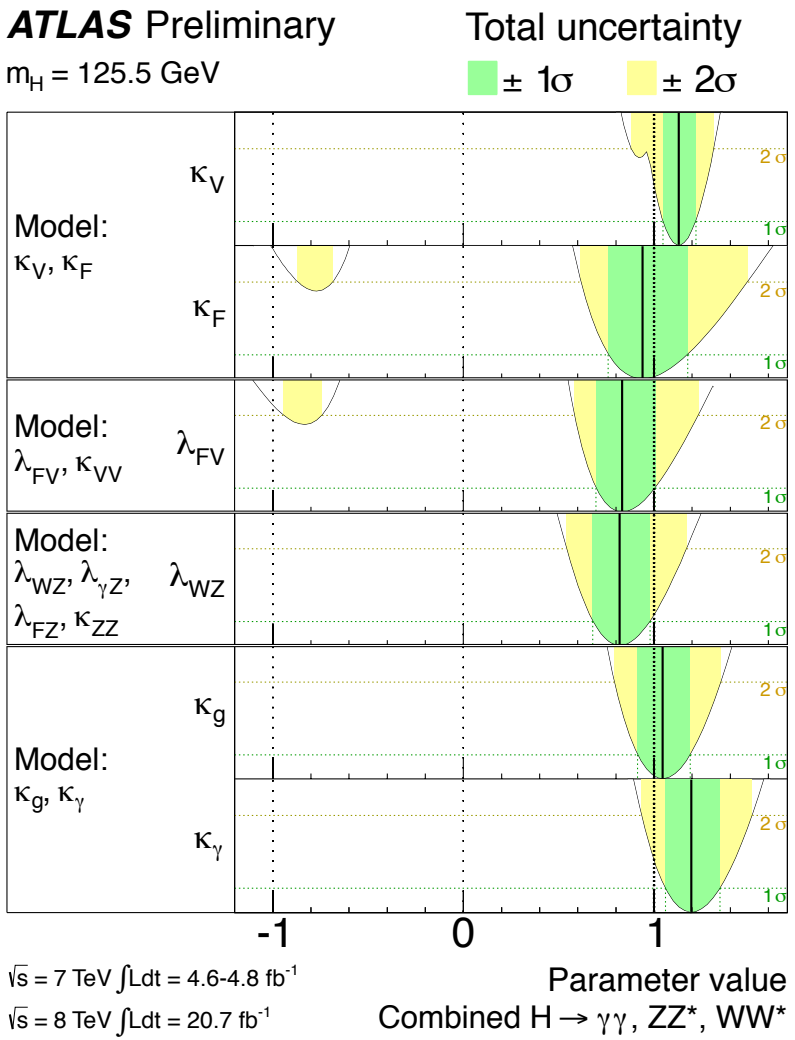

$$\lambda_{FV} = \frac{\kappa_{Fermion}}{\kappa_{VectorBoson}}\ ;\ \lambda_{WZ} = \frac{\kappa_W}{\kappa_Z} = 1$$ If custodial symmetry

Thank you for your attention !

BACKUP

Pile up

- Pile-up is a challenge: above designed value (50 ns bunch crossing)
- Instantaneous luminosity up to $7.7 \times 10^{33} cm^{-2} s^{-1}$
- ≈90% of delivered collisions used in the analyses

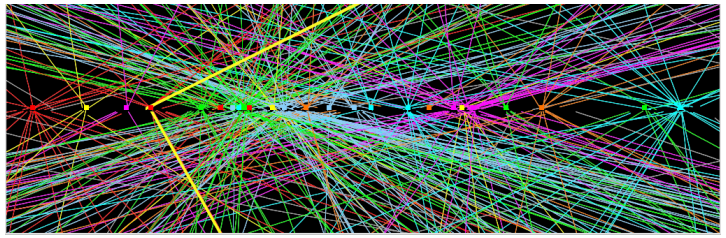

Z→μμ with 25 reconstructed interaction vertices

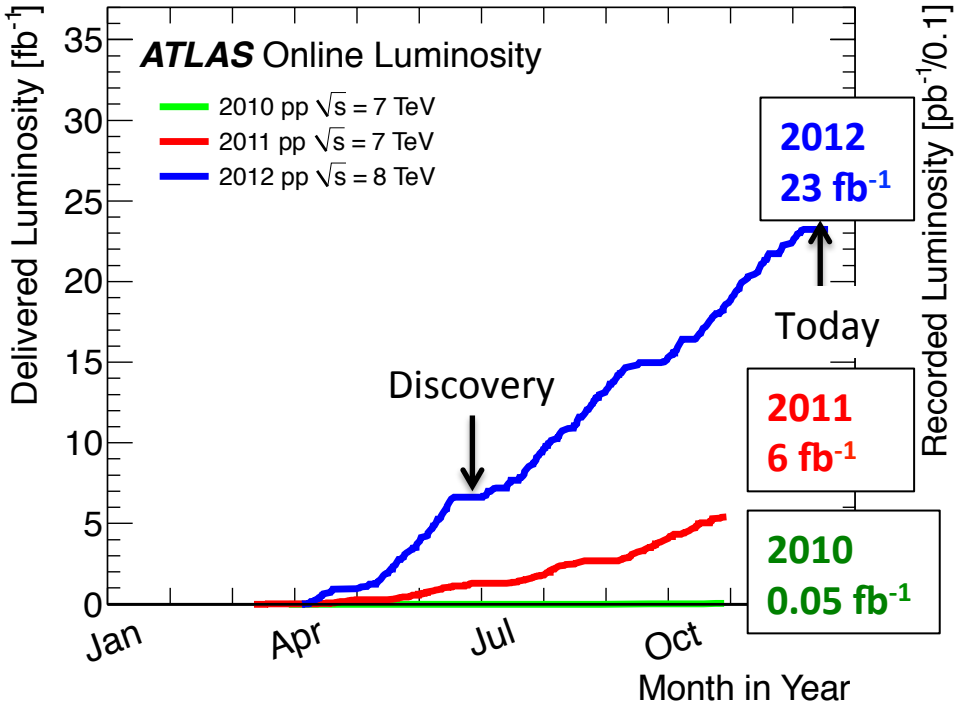

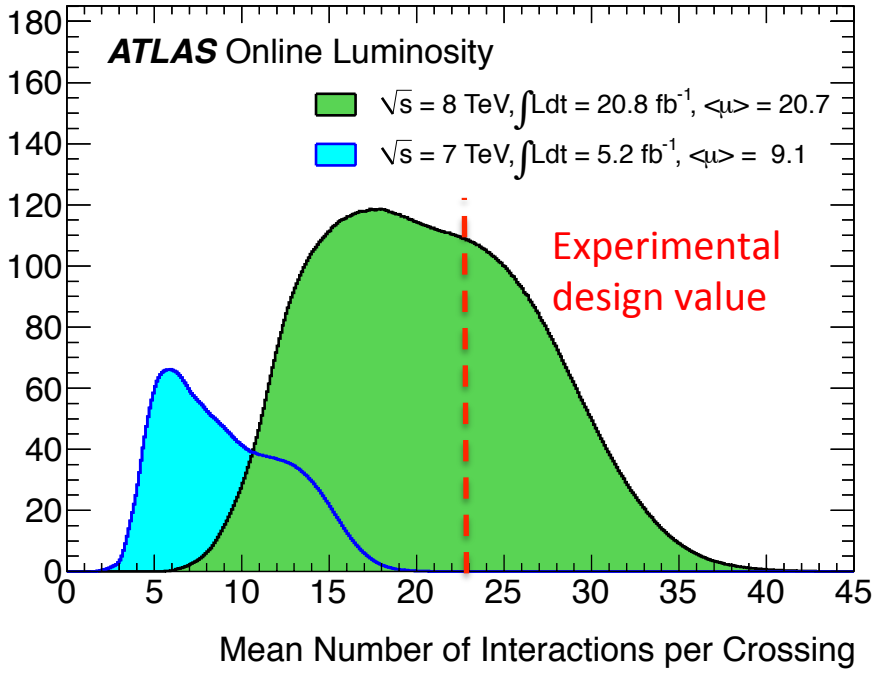

→ Many challenges to meet at the trigger and performance level

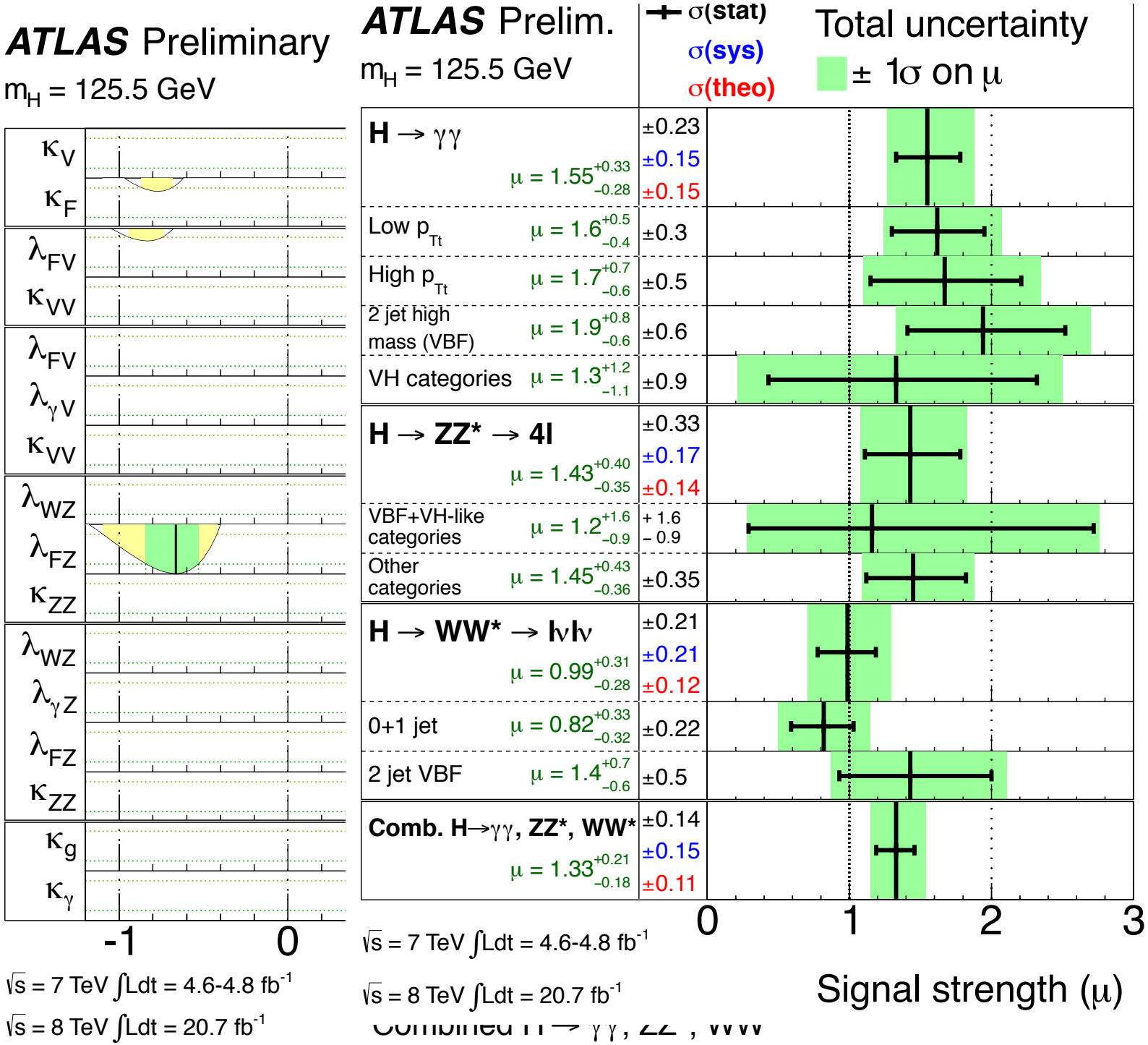
ATLAS Preliminary
m_H = 125.5 GeV
κ_V
κ_F
λ_FV
κ_VV
λ_FV
λ_γV
κ_VV
λ_WZ
λ_FZ
κ_ZZ
λ_WZ
λ_γZ
λ_FZ
κ_ZZ
κ_g
κ_γ
-1
0
√s = 7 TeV ∫Ldt = 4.6-4.8 fb^-1
√s = 8 TeV ∫Ldt = 20.7 fb^-1
ATLAS Prelim.
m_H = 125.5 GeV
σ(stat)
σ(sys)
σ(theo)
Total uncertainty
± 1σ on μ
H → γγ
μ = 1.55 +0.33 −0.28
±0.23
±0.15
±0.15
Low p_Tt
μ = 1.6 +0.5 −0.4
±0.3
High p_Tt
μ = 1.7 +0.7 −0.6
±0.5
2 jet high mass (VBF)
μ = 1.9 +0.8 −0.6
±0.6
VH categories
μ = 1.3 +1.2 −1.1
±0.9
H → ZZ* → 4l
μ = 1.43 +0.40 −0.35
±0.33
±0.17
±0.14
VBF+VH-like categories
μ = 1.2 +1.6 −0.9
+ 1.6
− 0.9
Other categories
μ = 1.45 +0.43 −0.36
±0.35
H → WW* → lνlν
μ = 0.99 +0.31 −0.28
±0.21
±0.21
±0.12
0+1 jet
μ = 0.82 +0.33 −0.32
±0.22
2 jet VBF
μ = 1.4 +0.7 −0.6
±0.5
Comb. H→γγ, ZZ*, WW*
μ = 1.33 +0.21 −0.18
±0.14
±0.15
±0.11
0
1
2
3
√s = 7 TeV ∫Ldt = 4.6-4.8 fb^-1
√s = 8 TeV ∫Ldt = 20.7 fb^-1
Signal strength (μ)

Statistical Treatment

- Profile likelihood ratio based test statistic

$$\lambda(\mu) = \tilde{q}_\mu = \begin{cases} -2\ln\dfrac{L(\mu,\hat{\hat{\theta}})}{L(\hat{\mu},\hat{\theta})} & 0 < \hat{\mu} < \mu \\ 0 & \hat{\mu} \geq \mu \\ -2\ln\dfrac{L(\mu,\hat{\hat{\theta}})}{L(0,\hat{\hat{\theta}}(0))} & \hat{\mu} < 0 \end{cases}$$

Distribution of λ for μ_{S+B} and μ_B hypothesis

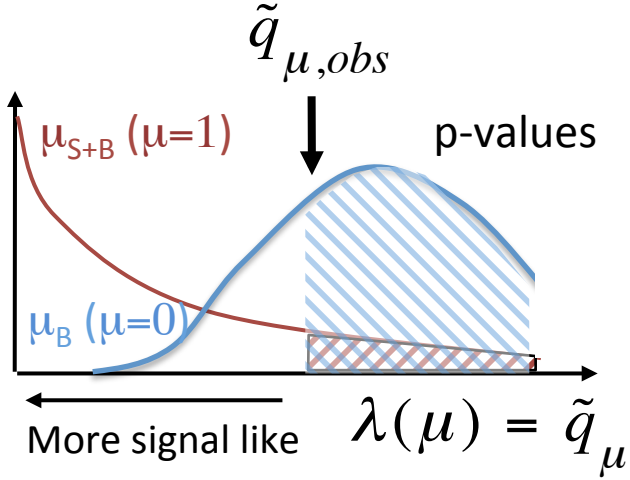

- p_0: probability of the background fluctuating beyond the observation in the data at a particular m_H

$$p_0 = p_{\mu=0} = \int_{\tilde{q}_{\mu,obs}}^{\infty} f(\lambda_{\mu=0})\,df$$

- To be translated into number of standard deviations from the background-only hypothesis or significance $Z = \Phi^{-1}(1 - p_0)$, where Φ^{-1} is the standard Gaussian quantile

	p_0	Z
Evidence	1.3×10^{-3}	3σ
Discovery	2.9×10^{-7}	5σ

- For mass measurement, both m_H and μ are free parameters:

$$\lambda(\mu) \rightarrow \lambda(\mu, m_H)$$

Categorisation

Both unconverted:

- Central
- Rest

At least one converted

- Central
- Transition
- Rest

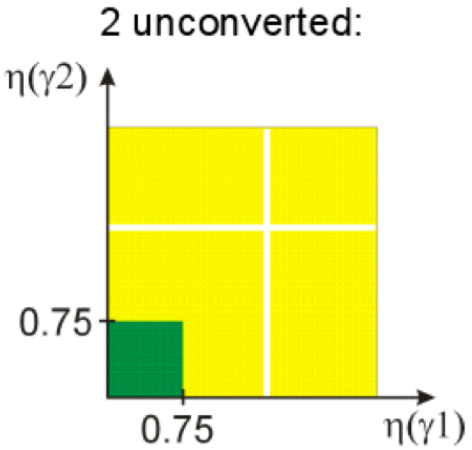

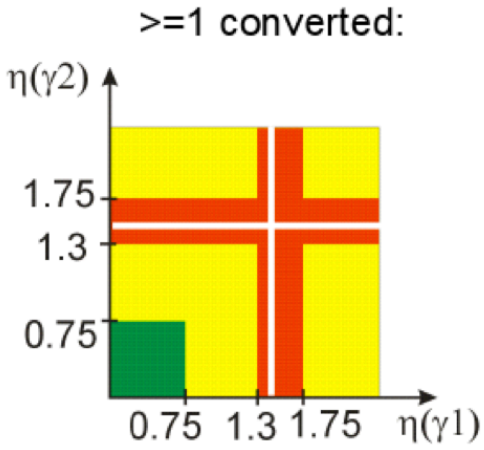

Resolution:

Good
Medium
Poor

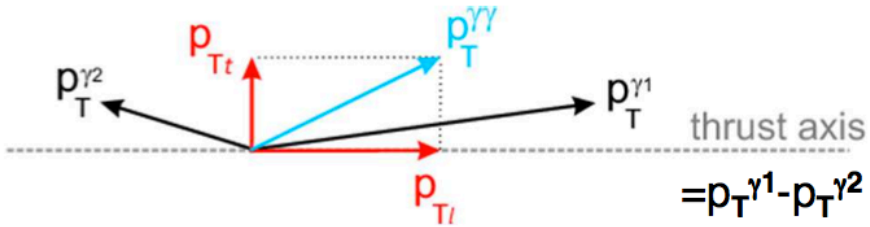

Variable p_{Tt} is strongly correlated with diphoton p_T but has better detector resolution and retains a monotically falling invariant mass for background

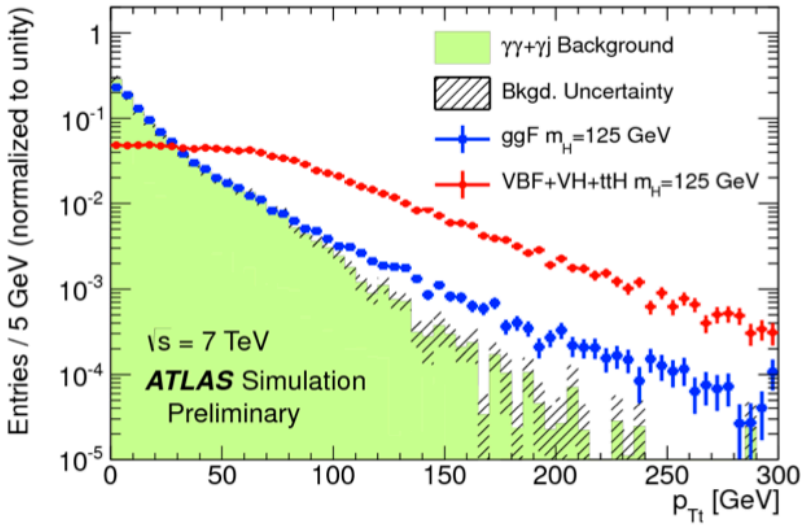

Vector Boson Fusion selection

- Boosted Decision Tree (BDT):
  - Combines of 8 discriminating variables exploiting the VBF topology: 2 forward jets and little hadronic activity between the 2 jets

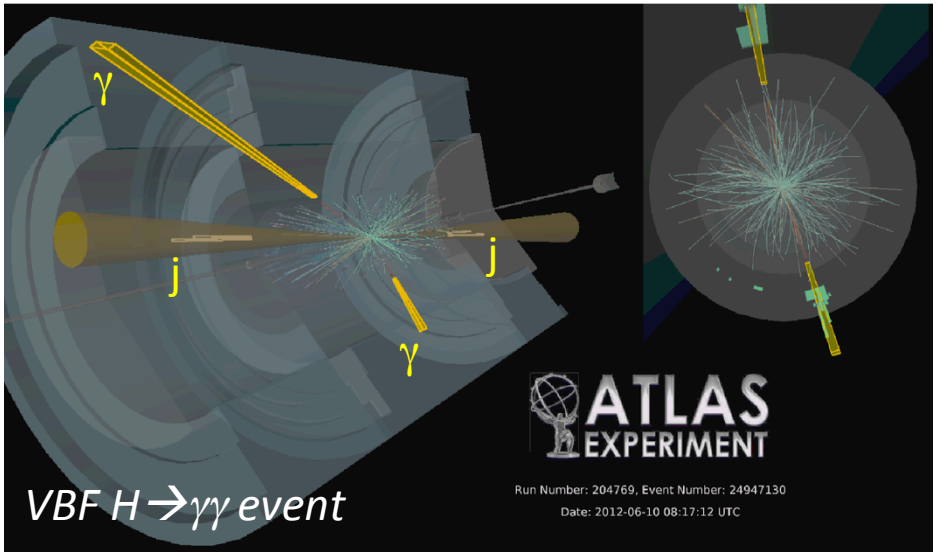

  - Invariant mass of the two leading jets m_{jj}
  - Their pseudorapidity η_{j1} and η_{j2}
  - Their pseudorapidity separation $\Delta\eta_{jj}$
  - p_{Tt} of the diphoton system
  - Azimuthal angle difference between the diphoton and the dijet systems $\Delta\phi_{\gamma\gamma;jj}$
  - Diphoton system pseudorapidity in the frame of the tagging jet pseudorapidity

$$\eta^* = \eta_{\gamma\gamma} - \frac{\eta_{j1}+\eta_{j2}}{2}$$

  - Minimal ΔR between one of the photons and one of the two leading jets $\Delta R^{\gamma j}_{\mathrm{min}}$

VBF and VH categories

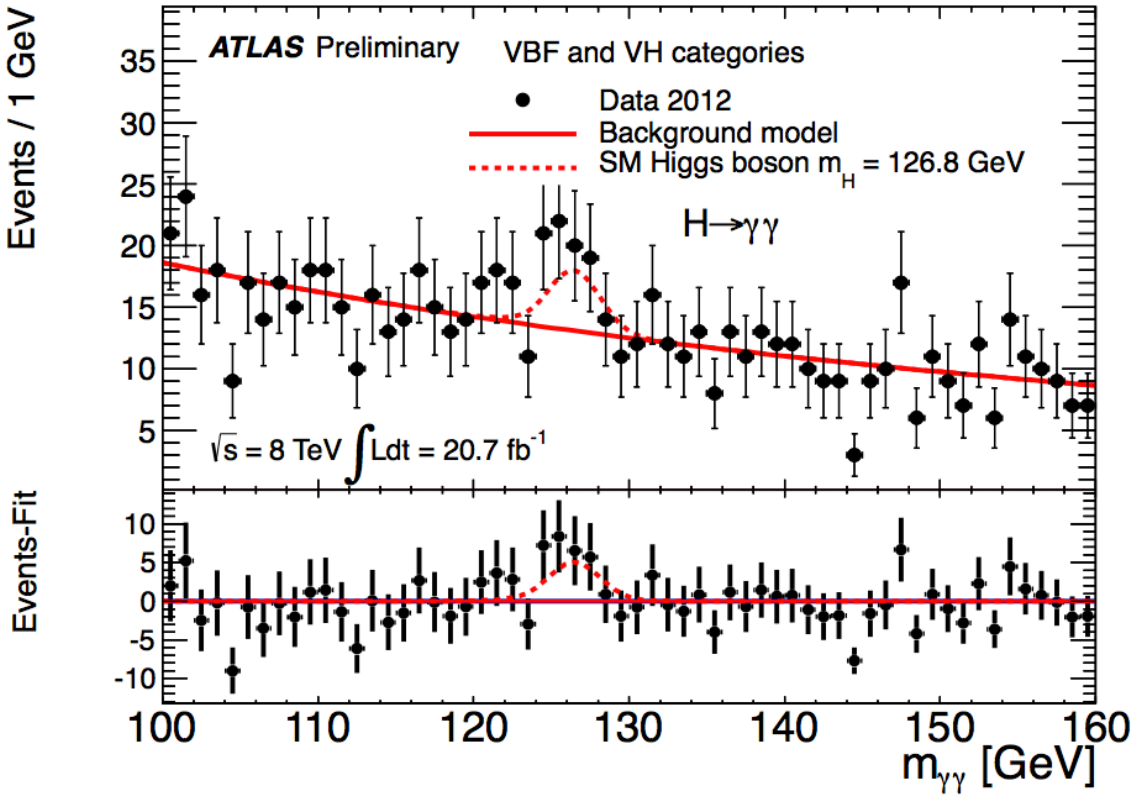

Systematics comparison

H→γγ mass systematic uncertainties

Absolute energy scale **from Z→ee**	0.3%
Uncertainties on upstream material simulation	0.3%
Pre-sampler energy scale	0.1%
Non-linearity of EM calo electronics	0.15%
Conversion fraction	0.1%
Relative calibration of first and second sampling	0.2%
Lateral leakage corrections	0.1%

+other smaller effects
Total systematic error is 0.55% (0.7 GeV)

4l mass measurement
dominated by the 4μ channel

Muon momentum scale	0.2%
Electron energy scale (4e)	0.4%
Low E_T electrons	0.1%

Possible local detector biases checked event by event

ID and MS measurements also checked separately

Yield Systematics

Systematic uncertainties	Value(%)			Constraint
Luminosity	±3.6			
Trigger	±0.5			
Photon Identification	±2.4			Log-normal
Isolation	±1.0			
Photon Energy Scale	±0.25			
Branching ratio	±5.9% − ±2.1% (m_H = 110 - 150 GeV)			Asymmetric Log-normal
Scale	ggF: $^{+7.2}_{-7.8}$	VBF: $^{+0.2}_{-0.2}$	WH: $^{+0.2}_{-0.6}$	Asymmetric
	ZH: $^{+1.6}_{-1.5}$	ttH: $^{+3.8}_{-9.3}$		Log-normal
PDF+α_s	ggF: $^{+7.5}_{-6.9}$	VBF: $^{+2.6}_{-2.7}$	WH: ±3.5	Asymmetric
	ZH: ±3.6	ttH: ±7.8		Log-normal
Theory cross section on ggF	Tight high-mass two-jet:		±48	Log-normal
	Loose high-mass two-jet:		±28	
	Low-mass two-jet:		±30	

Systematic uncertainties	Category	Value(%)			Constraint
Underlying Event	Tight high-mass two-jet	ggF: ±8.8	VBF: ±2.0	VH, ttH: ±8.8	Log-normal
	Loose high-mass two-jet	ggF: ±12.8	VBF: ±3.3	VH, ttH: ±12.8	
	Low-mass two-jet	ggF: ±12	VBF: ±3.9	VH, ttH: ±12	
Jet Energy Scale	Low p_{Tt}	ggF: −0.1	VBF: −1.0	Others: −0.1	Gaussian
	High p_{Tt}	ggF: −0.7	VBF: −1.3	Others: +0.4	
	Tight high-mass two-jet	ggF: +11.8	VBF: +6.7	Others: +20.2	
	Loose high-mass two-jet	ggF: +10.7	VBF: +4.0	Others: +5.7	
	Low-mass two-jet	ggF: +4.7	VBF: +2.6	Others: 1.4	
	$E_{\mathrm{T}}^{\mathrm{miss}}$significance	ggF: 0.0	VBF: 0.0	Others: 0.0	
	one-lepton	ggF: 0.0	VBF: 0.0	Others: −0.1	
Jet Energy Resolution	Low p_{Tt}	ggF: 0.0	VBF: 0.2	Others: 0.0	Gaussian
	High p_{Tt}	ggF: −0.2	VBF: 0.2	Others: 0.6	
	Tight high-mass two-jet	ggF: 3.8	VBF: −1.3	Others: 7.0	
	Loose high-mass two-jet	ggF: 3.4	VBF: −0.7	Others: 1.2	
	Low-mass two-jet	ggF: 0.5	VBF: 3.4	Others: −1.3	
	$E_{\mathrm{T}}^{\mathrm{miss}}$significance	ggF: 0.0	VBF: 0.0	Others: 0.0	
	one-lepton	ggF: −0.9	VBF: −0.5	Others: −0.1	
$\eta^{\star}$ modelling		Tight high-mass two-jet: +7.6			Gaussian
		Loose high-mass two-jet: +6.2			
Dijet angular modelling		Tight high-mass two-jet: +12.1			Gaussian
		Loose high-mass two-jet: +8.5			
Higgs p_{T}		Low p_{Tt}: +1.3			Gaussian
		High p_{Tt}: −10.2			
		Tight high-mass two-jet: −10.4			
		Loose high-mass two-jet: −8.5			
		Low-mass two-jet: −12.5			
		$E_{\mathrm{T}}^{\mathrm{miss}}$significance: −2.0			
		one-lepton : −4.0			
Material Mismodelling		Unconv: −4.0	Conv: +3.5		Gaussian
JVF	Loose High-mass two-jet	ggF: −1.2	VBF: −0.3	Others: −1.2	Gaussian
	Low-mass two-jet	ggF: −2.3	VBF: −2.4	Others: −2.3	
$E_{\mathrm{T}}^{\mathrm{miss}}$	$E_{\mathrm{T}}^{\mathrm{miss}}$significance	ggF: +66.4	VBF: +30.7	VH, ttH: +1.2	Gaussian
e reco and identification		one-lepton: < 1			Gaussian
e Escale and resolution		one-lepton: < 1			Gaussian
μ reco, ID resolution		one-lepton: < 1			Gaussian
μ spectrometer resolution		one-lepton: 0			Gaussian

Migration Systematics

Profile likelihood statistic test :

$$q_\mu = -2\ln\frac{L(\mu,\hat{\hat{\theta}})}{L(\hat{\mu},\hat{\theta})}$$

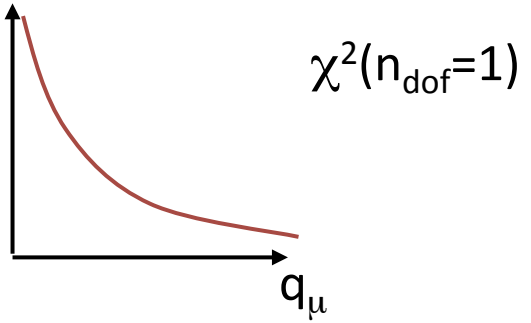

We want the cases μ tested>μ to be signal like instead of populating the χ2

"one-sided" definition :

$$q_\mu = \begin{cases} -2\ln\dfrac{L(\mu,\hat{\hat{\theta}})}{L(\hat{\mu},\hat{\theta})} & \hat{\mu} \le \mu \\ 0 & \hat{\mu} > \mu \end{cases}$$

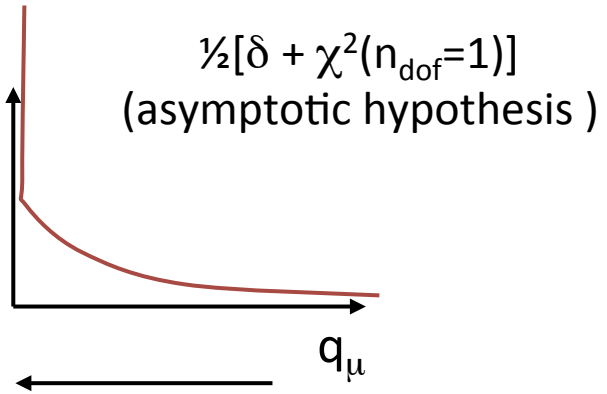

The intensity of higgs signal cannot be negative so we set μ tested to 0 when negative values are probed

"qmuTilda" used in Higgs analysis :

$$\tilde{q}_\mu = \begin{cases} -2\ln\dfrac{L(\mu,\hat{\hat{\theta}})}{L(\hat{\mu},\hat{\theta})} & 0 < \hat{\mu} < \mu \\ 0 & \hat{\mu} \ge \mu \\ -2\ln\dfrac{L(\mu,\hat{\hat{\theta}})}{L(0,\hat{\hat{\theta}}(0))} & \hat{\mu} < 0 \end{cases}$$

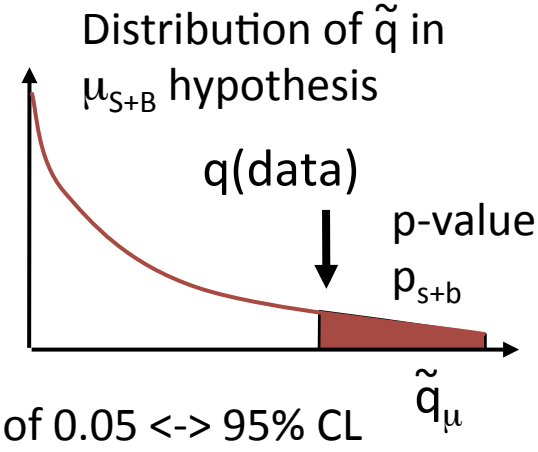

p-value of 0.05 <-> 95% CL

CLs

CLs is used to be less sensitive to the background fluctuations than CLs+b
Evaluates the probability to have data compatible with the signal hypothesis, knowing the background

$$p_S = \frac{p_{S+B}}{1-p_B} = \frac{1-CL_{S+B}}{CL_B} \qquad CL_S = 1-p_S = 1-\left(\frac{1-CL_{S+B}}{CL_B}\right)$$

CLb is the test for the background only hypothesis : μ=0 : $-2\ln\frac{L(\mu=0,\hat{\hat{\theta}})}{L(\hat{\mu},\hat{\theta})}$

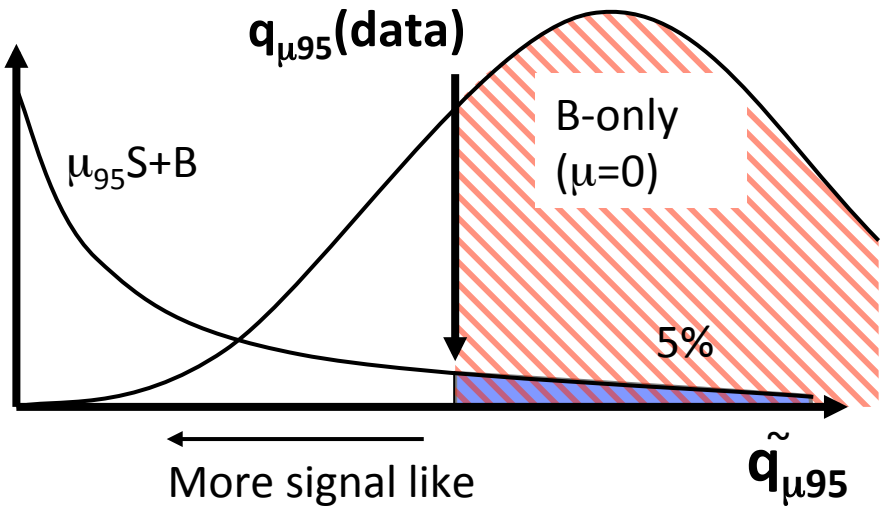

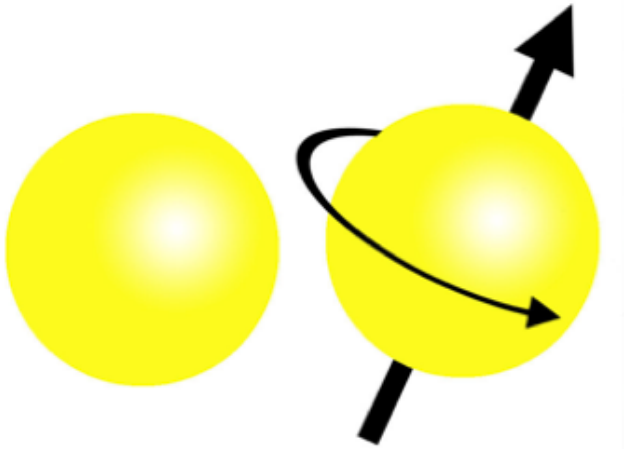

SPIN

Wigner's functions

$$d^{j}_{m',m} = (-1)^{m-m'} d^{j}_{m,m'} = d^{j}_{-m,-m'}$$

2×2

$+2,+2$	$+2,+1$	$+2,0$	$+2,-1$	$+2,-2$
1	$1/2$	$\sqrt{3/14}$	$1/\sqrt{14}$	$1/70$
$+1,+2$	$1/2$	$\sqrt{4/7}$	$3/\sqrt{70}$	$\sqrt{8/35}$
$0,+2$	$\sqrt{3/14}$	$1/2$	$3/\sqrt{70}$	$\sqrt{18/35}$
$-1,+2$	$1/\sqrt{14}$	$3/\sqrt{70}$	$1/2$	$\sqrt{8/35}$
$-2,+2$	$1/70$	$\sqrt{8/35}$	$\sqrt{18/35}$	$\sqrt{8/35}$

$+1,+2$	$+1,+1$	$+1,0$	$+1,-1$	$+1,-2$
$1/2$	$1/2$	$\sqrt{3/14}$	$1/\sqrt{14}$	$1/70$
$-1/2$	$\sqrt{4/7}$	$-1/2$	$3/\sqrt{70}$	$\sqrt{8/35}$
$\sqrt{3/14}$	$-1/2$	$-\sqrt{4/7}$	$1/2$	$\sqrt{8/35}$
$1/\sqrt{14}$	$3/\sqrt{70}$	$1/2$	$-\sqrt{4/7}$	$\sqrt{18/35}$
$1/70$	$\sqrt{8/35}$	$\sqrt{18/35}$	$\sqrt{8/35}$	$1/2$

$0,+2$	$0,+1$	$0,0$	$0,-1$	$0,-2$
$\sqrt{3/14}$	$\sqrt{4/7}$	0	$-\sqrt{4/7}$	$-\sqrt{3/14}$
$1/2$	0	$-1/2$	0	$1/2$
$\sqrt{3/14}$	$-\sqrt{4/7}$	0	$\sqrt{4/7}$	$-\sqrt{3/14}$
$1/2$	0	$-1/2$	0	$1/2$
$\sqrt{3/14}$	$\sqrt{4/7}$	0	$-\sqrt{4/7}$	$\sqrt{3/14}$

$-1,+2$	$-1,+1$	$-1,0$	$-1,-1$	$-1,-2$
$1/14$	$3/10$	$3/7$	$1/5$	$1/70$
$3/7$	$1/5$	$-1/14$	$-3/10$	$\sqrt{8/35}$
$3/7$	$-1/5$	$-1/14$	$3/10$	$\sqrt{18/35}$
$1/14$	$-3/10$	$3/7$	$-1/5$	$\sqrt{8/35}$
$1/70$	$-1/10$	$2/7$	$-2/5$	$1/5$

$-2,+2$	$-2,+1$	$-2,0$	$-2,-1$	$-2,-2$
$1/70$	$1/10$	$2/7$	$2/5$	$1/5$
$8/35$	$2/5$	$1/14$	$-1/10$	$-1/5$
$18/35$	0	$-2/7$	0	$1/5$
$8/35$	$-2/5$	$1/14$	$1/10$	$-1/5$
$1/70$	$-1/10$	$2/7$	$-2/5$	$1/5$

$3/2\times3/2$

$+3/2,+3/2$	$+3/2,+1/2$	$+3/2,-1/2$	$+3/2,-3/2$
1	$1/2$	$1/5$	$1/20$
$+1/2,+3/2$	$1/2$	$3/5$	$9/20$
$-1/2,+3/2$	$1/5$	$-1/2$	$9/20$
$-3/2,+3/2$	$1/20$	$-1/4$	$-9/20$

$+1/2,+3/2$	$+1/2,+1/2$	$+1/2,-1/2$	$+1/2,-3/2$
$1/2$	$1/2$	$3/10$	$1/4$
$-1/2$	$3/10$	$1/5$	$9/20$
$3/10$	$-1/5$	$-1/2$	$1/20$
$1/4$	$-9/20$	$-1/4$	$-1/20$

$-1/2,+3/2$	$-1/2,+1/2$	$-1/2,-1/2$	$-1/2,-3/2$
$1/5$	$3/10$	$3/5$	$1/5$
$3/5$	$-2/5$	0	$-1/2$
$3/10$	$-1/5$	$-1/2$	$3/10$
$1/4$	$-9/20$	$-1/4$	$-1/20$

$-3/2,+3/2$	$-3/2,+1/2$	$-3/2,-1/2$	$-3/2,-3/2$
$1/20$	$1/4$	$9/20$	$1/4$
$9/20$	$1/4$	$-1/20$	$-1/4$
$-1/20$	$-1/4$	$-9/20$	$1/4$
$1/4$	$-9/20$	$-1/4$	$9/20$

$$d^{1}_{0,0} = \cos\theta \qquad d^{1/2}_{1/2,1/2} = \cos\frac{\theta}{2} \qquad d^{1}_{1,1} = \frac{1+\cos\theta}{2}$$

$$d^{1/2}_{1/2,-1/2} = -\sin\frac{\theta}{2} \qquad d^{1}_{1,0} = -\frac{\sin\theta}{\sqrt{2}}$$

$$d^{1}_{1,-1} = \frac{1-\cos\theta}{2}$$

$$d^{3/2}_{3/2,3/2} = \frac{1+\cos\theta}{2}\cos\frac{\theta}{2}$$

$$d^{3/2}_{3/2,1/2} = -\sqrt{3}\frac{1+\cos\theta}{2}\sin\frac{\theta}{2} \qquad d^{2}_{2,2} = \left(\frac{1+\cos\theta}{2}\right)^2$$

$$d^{3/2}_{3/2,-1/2} = \sqrt{3}\frac{1-\cos\theta}{2}\cos\frac{\theta}{2} \qquad d^{2}_{2,1} = -\frac{1+\cos\theta}{2}\sin\theta$$

$$d^{3/2}_{3/2,-3/2} = -\frac{1-\cos\theta}{2}\sin\frac{\theta}{2} \qquad d^{2}_{2,0} = \frac{\sqrt{6}}{4}\sin^2\theta \qquad d^{2}_{1,1} = \frac{1+\cos\theta}{2}(2\cos\theta - 1)$$

$$d^{3/2}_{1/2,1/2} = \frac{3\cos\theta - 1}{2}\cos\frac{\theta}{2} \qquad d^{2}_{2,-1} = -\frac{1-\cos\theta}{2}\sin\theta \qquad d^{2}_{1,0} = -\sqrt{\frac{3}{2}}\sin\theta\cos\theta$$

$$d^{3/2}_{1/2,-1/2} = -\frac{3\cos\theta + 1}{2}\sin\frac{\theta}{2} \qquad d^{2}_{2,-2} = \left(\frac{1-\cos\theta}{2}\right)^2 \qquad d^{2}_{1,-1} = \frac{1-\cos\theta}{2}(2\cos\theta + 1) \qquad d^{2}_{0,0} = \left(\frac{3}{2}\cos^2\theta - \frac{1}{2}\right)$$

Summary of Analysis Setup (1)

- 1Dx1D fit stands for fit of $m_{\gamma\gamma}$ and $\cos\theta^*$
- Selection:
  - $p_{T1}/m_{\gamma\gamma} > 0.35$, $p_{T2}/m_{\gamma\gamma} > 0.25$
  - $m_{\gamma\gamma}$ in [105;160] → raised lower bound from 100 to 105 to avoid trigger turn on effects from relative p_T cuts
- Signal models :
  - $m_{\gamma\gamma}$ pdf: from MC, common to spin 0 and spin 2
  - $\cos\theta^*$ pdf: switch from 20 to 10 bins to be presented in this talk

Signal Spin 2

(for the moment 100% gg)
from JHU 2^+ MC after $p_{T\gamma\gamma}$ reweighting

⇒ systematic: difference with non-reweighted MC sample, treated as Gaussian-constrained nuisance parameter

Signal Spin 0

from PowhegPythia (ggH,VBF) + Pythia (VH,ttH) after applying the interference correction (for ggH)

⇒ systematic from interference, preliminary results to be presented in this talk

Summary of Analysis Setup (2)

→ $m_{\gamma\gamma}$ fit in the 3 regions
→ $m_{\gamma\gamma}$ x cosθ* fit in the signal region

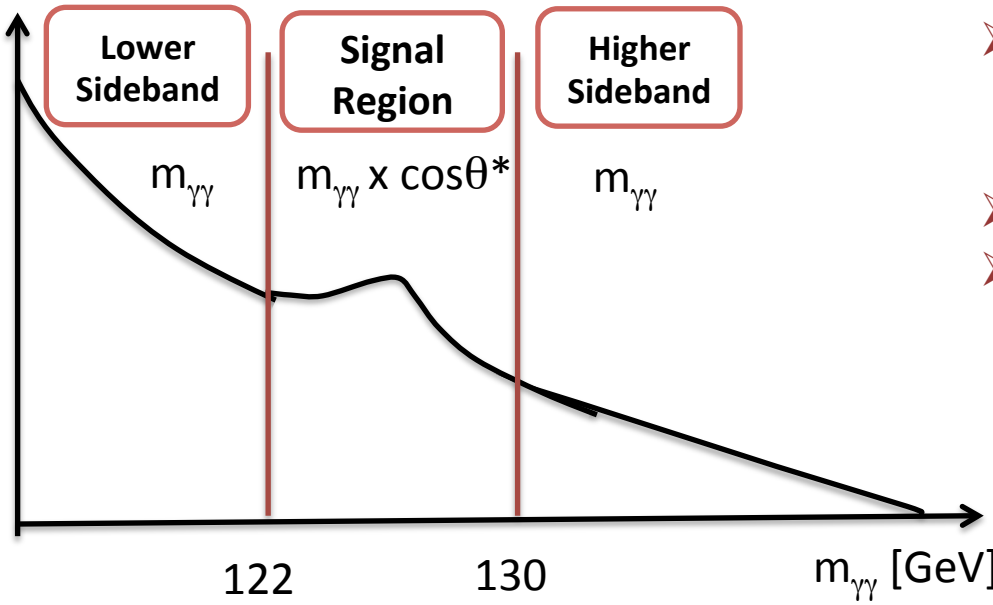

cosθ* pdf: several possibilities

Taking directly the mass sidebands

- Background model:
- Mass fit performed with an analytical function passing spurious signal requirements (Bernstein 5)
- Cosθ* pdfs done with HistFactory
- N_{bkg} and μ are obtained from the same fit (no sidebands pre-fit to determine the bkg in the signal region)

Systematics

- Spin-0 Cosθ* signal modelling (from MC) :
  - Interference between the signal gg → H → γγ and the non-resonant background gg → γγ
  - (photon identification efficiencies in different pseudorapidity and the systematic uncertainty on the photon energy scale are negligible)
  - (transverse momentum NNLL+NLO)
- Spin-2 Cosθ* signal modelling (from MC, reweighted the leading-order prediction of the pT spectrum generated by parton shower in JHU to the Standard Model prediction from POWHEG (SM))
  - conservative systematic uncertainty, taken as the full magnitude of the correction
  - No interference considered because model dependant
- Cosθ* background modelling (normalised distribution of | cos θ*| when summing the events in both mass sidebands) :
  - Limited statistics in the sidebands
  - small remaining correlations between mγγ and | cos θ*|, observed in high statistics MC samples

Sum in quadrature, uncorrelated between bins

$M_{\gamma\gamma}$/cosθ* correlations

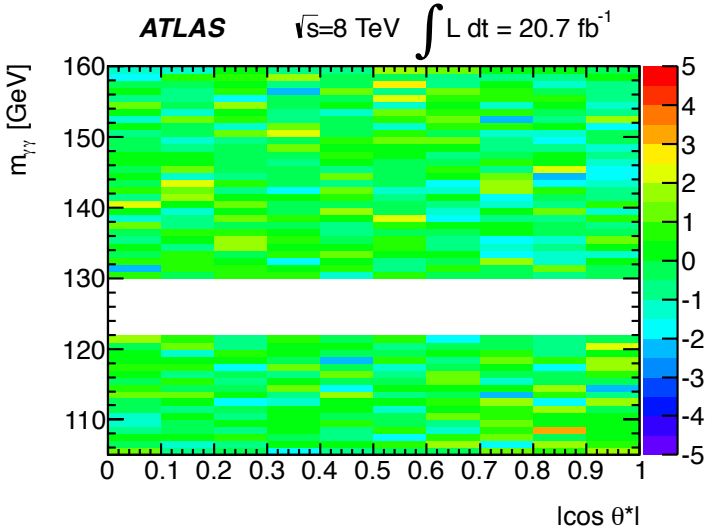

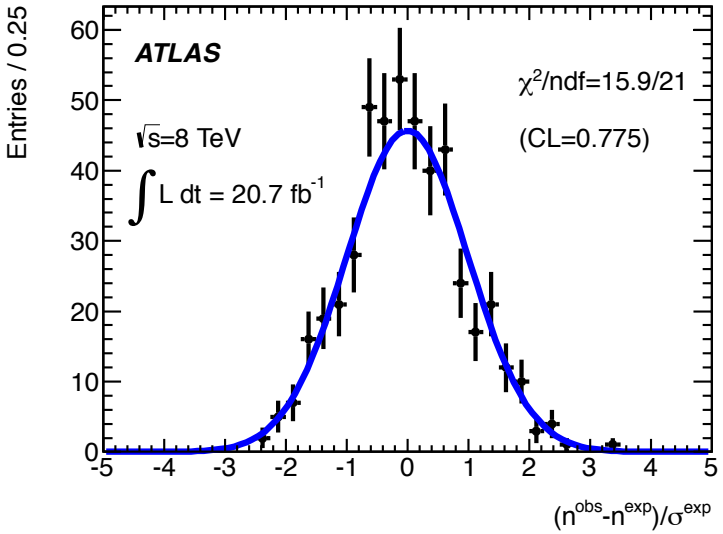

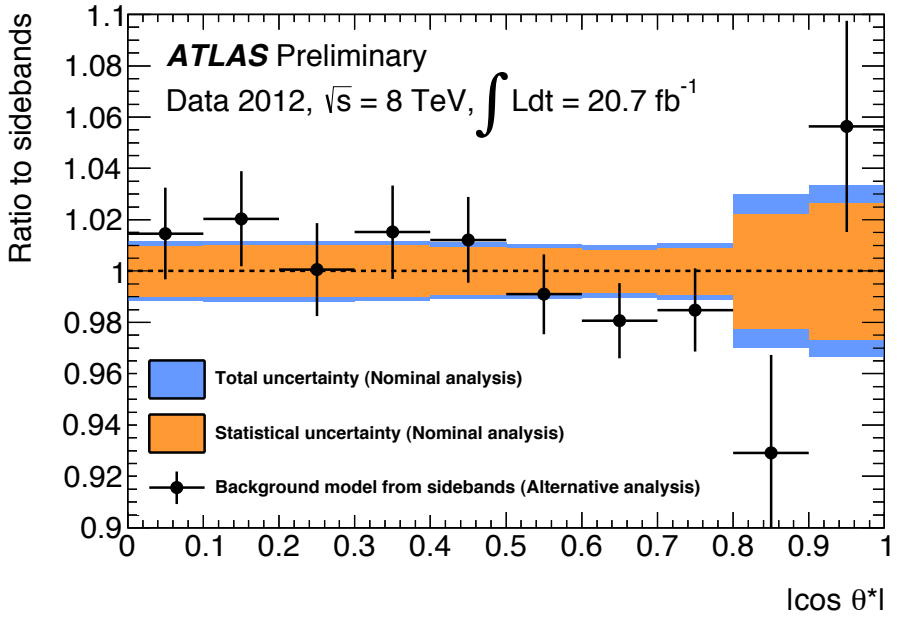


H